Radiation Stability of Multilayer Structures

Gary S. Was
University of Michigan

US Fusion Materials Science Program
Strategic Planning Meeting

University of California at Santa Barbara
August 26-30, 2002

MichiganEngineering

What is the composition and phase stability of multilayer structures under irradiation?

- Interface mixing
  - recoil implantation
  - displacement (cascade) mixing (DM)
  - radiation enhanced diffusion (RED)
  - radiation induced segregation (RIS)
- Phase stability
  - phase separation
  - phase formation
- Irradiation of multilayers
- Synthesis of multilayers

Displacement Mixing

In the atomistic model of thermal diffusion:

$$D = 1/6\ \lambda^2\Gamma,$$

λ= jump length, Γ = jump frequency.

The transport under irradiation is characterized by an effective diffusion coefficient:

$$D^* = 1/6R^2F$$

R = root-mean square displ. of an atom in the collision cascade,
F = atomic displacement rate in dpa/s.

F is estimated from the K-P displacement model:

$$F = \frac{dE/dx|_n\ \phi}{4\ E_{d,min}\ N}$$

yielding $D^* = \dfrac{R^2\, dE/dx|_n\, \phi}{24\, E_{d,min}\, N}$

Fick's 2nd law: $$\frac{\partial C}{\partial t} = -\nabla \cdot D\nabla C = -D\nabla^2 C \quad \text{for } D \neq f(C)$$

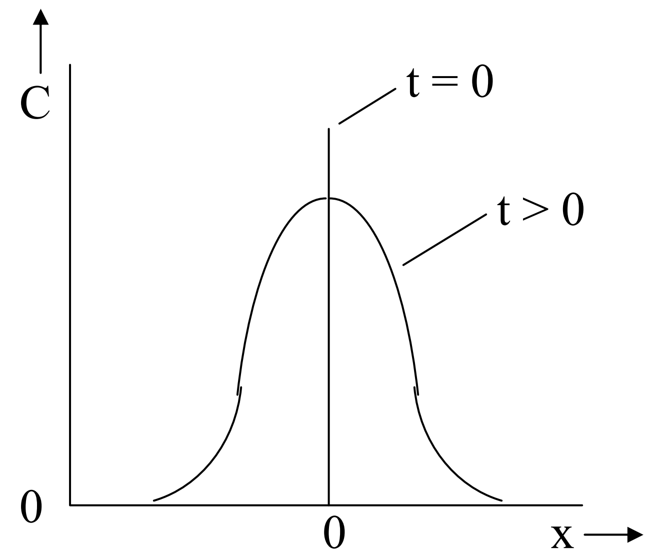

Thin film solution

for $|x|>0$, C-->0 as t-->0
for x=0, C-->1 as t-->0

and $$\int_{-\infty}^{\infty} C(x,t)\,dx = \alpha$$

$$C(x,t) = \frac{\alpha}{\sqrt{4\pi Dt}} \exp\left(\frac{-x^2}{4Dt}\right)$$

variance, $\sigma^2 = 4Dt$
std. deviation, $\sigma = (4Dt)^{1/2}$
FWHM = 2.35 σ

MichiganEngineering

So, given the expression for D*, the increment of FWHM due to cascade mixing is:

$$\Delta FWHM = 2.35\sqrt{4D^* t} \cong 5R\left[\frac{dE/dx|_n\ \phi t}{24E_{d,min}N}\right]^{1/2}$$

Note that broadening is proportional to $(\phi t)^{1/2}$

MichiganEngineering

Example

What dose of 150 keV Kr^+ on Ni marker in Al is required to produce a ΔFWHM of 10 nm?

$$\Delta FWHM = 10nm = 5R\left[\frac{dE/dx|_n\ \phi t}{24E_{d,min}N}\right]^{1/2}$$

For $dE/dx|n = N\sigma_s T$

$$\Delta FWHM = 10nm = 5R\left[\frac{\sigma\overline{T}(\phi t)}{24E_{d,min}}\right]^{1/2}$$

$\sigma \sim 10^{-16}\ cm^2$

$\sigma T \sim E_o = 150$ keV

$\sigma E_{d,min} \sim 15$ eV

$R \sim 1.5$ nm

then $\phi t = 6 \times 10^{14}\ i/cm^2$ for 150 keV Kr^+

for He^+ at 150 keV, $\phi t = 2.5 \times 10^{15}\ i/cm^2$

Marker Layer Experiments

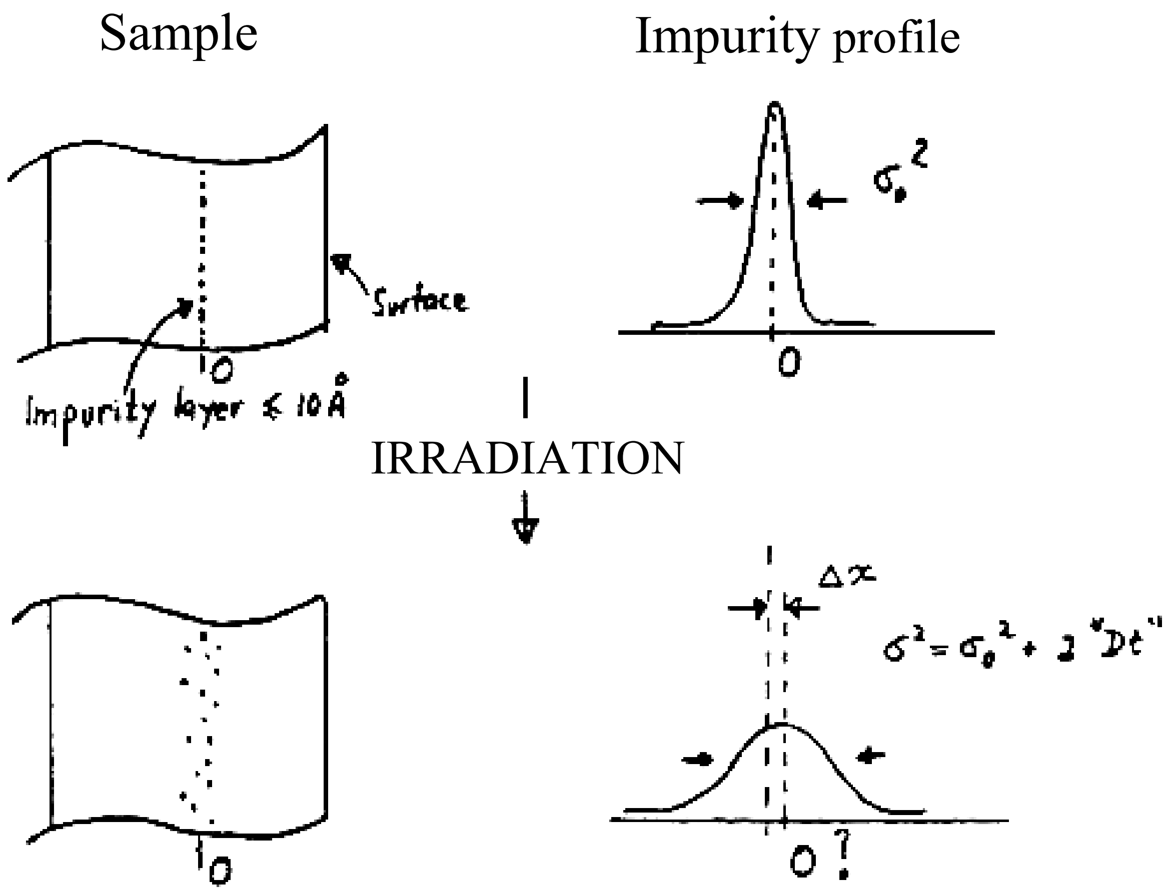

BM Paine in Ion Mixing and Surface Layer Alloying, Noyes, 1984, p. 26

Marker Broadening - Rutherford Backscattering Spectra

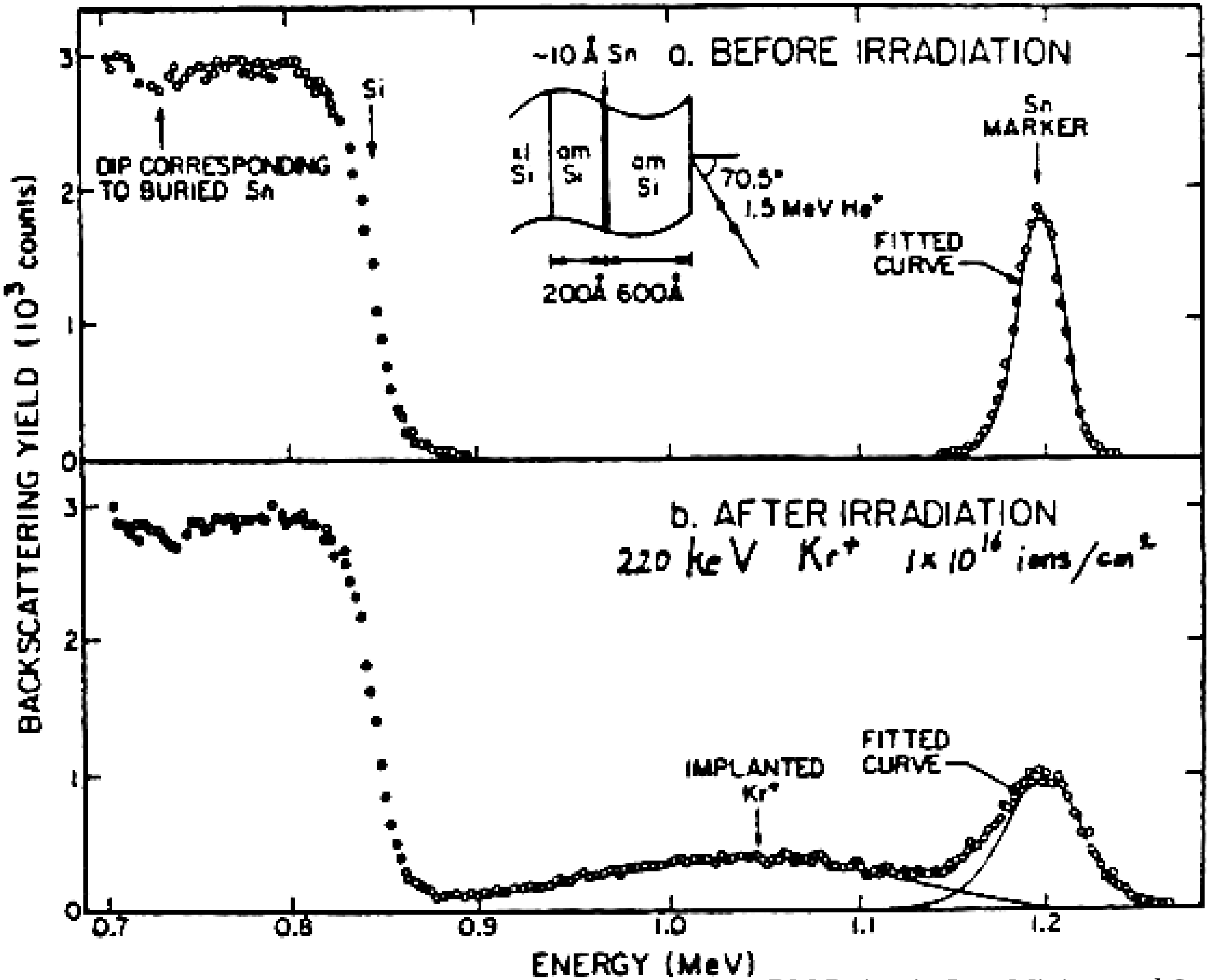

BM Paine in Ion Mixing and Surface Layer Alloying, Noyes, 1984, p. 26

Fluence dependence of marker broadening

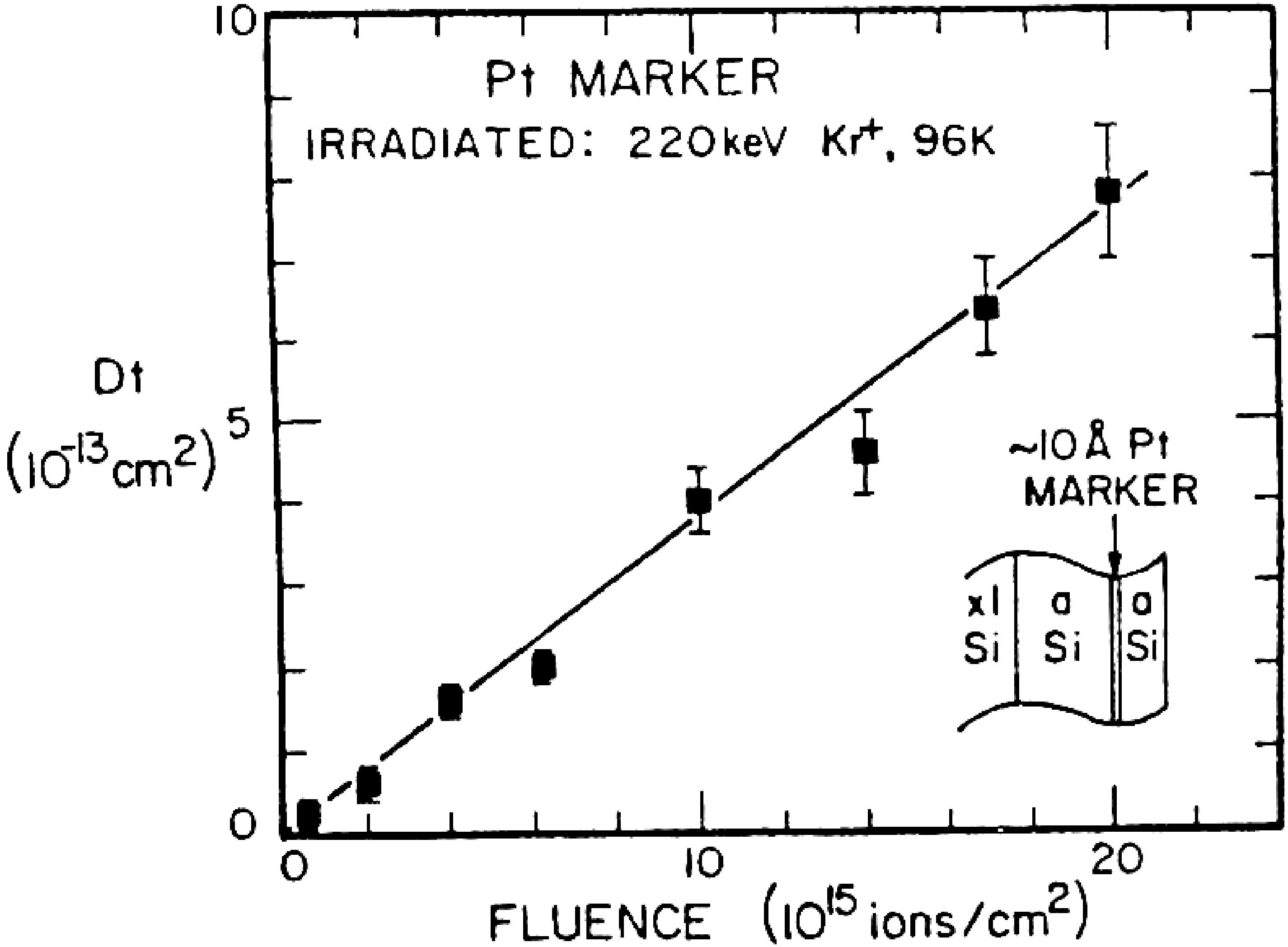

BM Paine in Ion Mixing and Surface Layer Alloying, Noyes, 1984, p. 26

Thin film of finite thickness (multilayer)

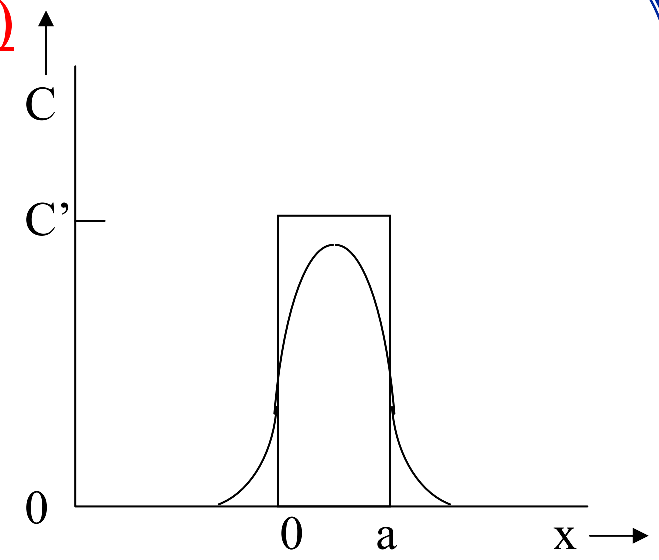

B.C. $C = C'$ for $0<x<a$, $t = 0$

$C = 0$ for $x<0$, $x>a$ at $t=0$

$$C(x,t) = \frac{C'}{2}\left[\operatorname{erf}\left(\frac{x}{\sqrt{4Dt}}\right) - \operatorname{erf}\left(\frac{x-a}{\sqrt{4Dt}}\right)\right]$$

In terms of experimentally measured spectra,

$$\sigma^2_{total} = \sigma^2_{unirrad} + \sigma^2_{mixing}$$
$$\sigma^2_{total} = \sigma^2_{unirrad} + 4Dt$$

Broadening of multilayers

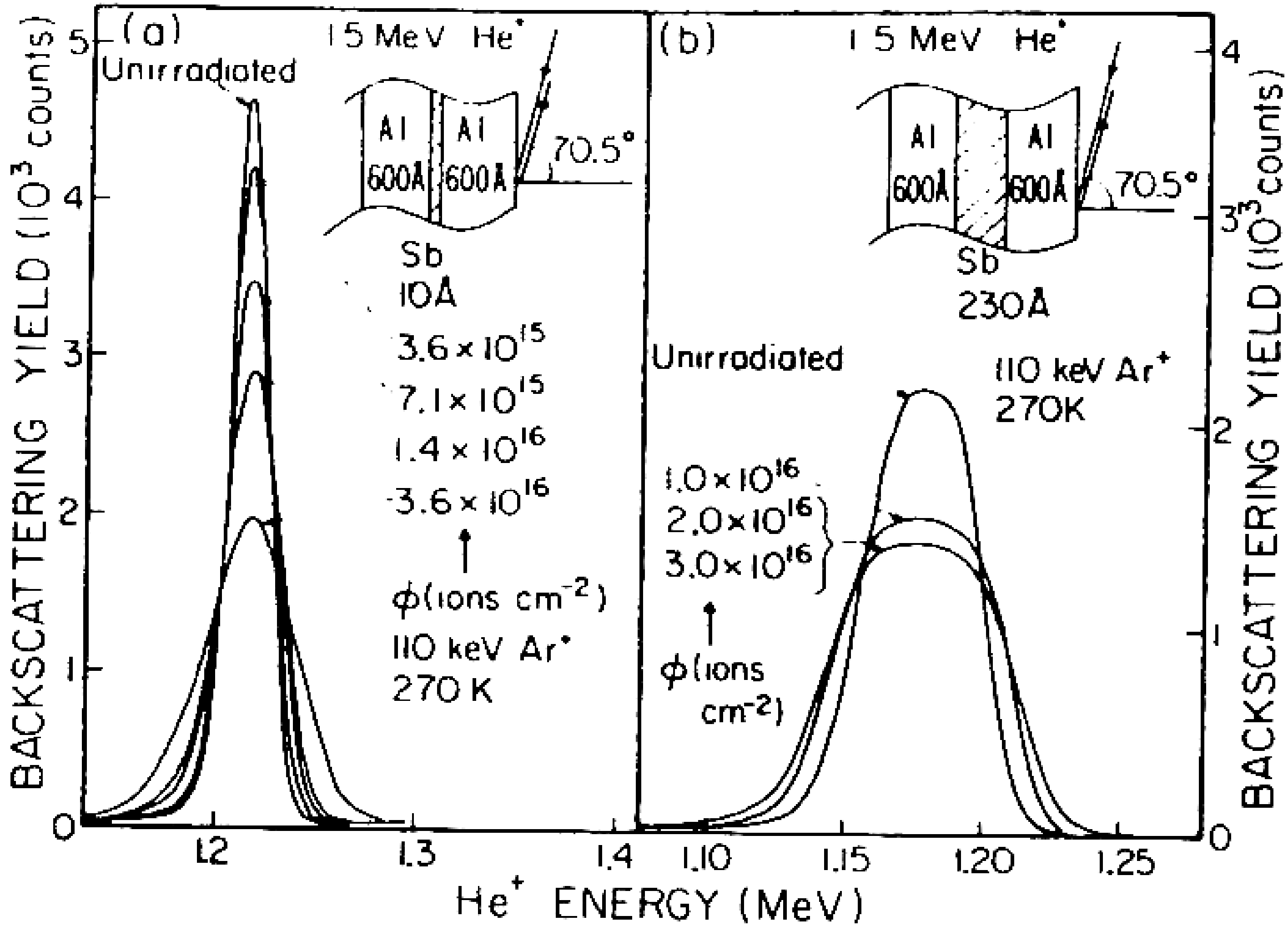

BM Paine et al., MRS Proc., 1982.

Dose dependence of interface spreading

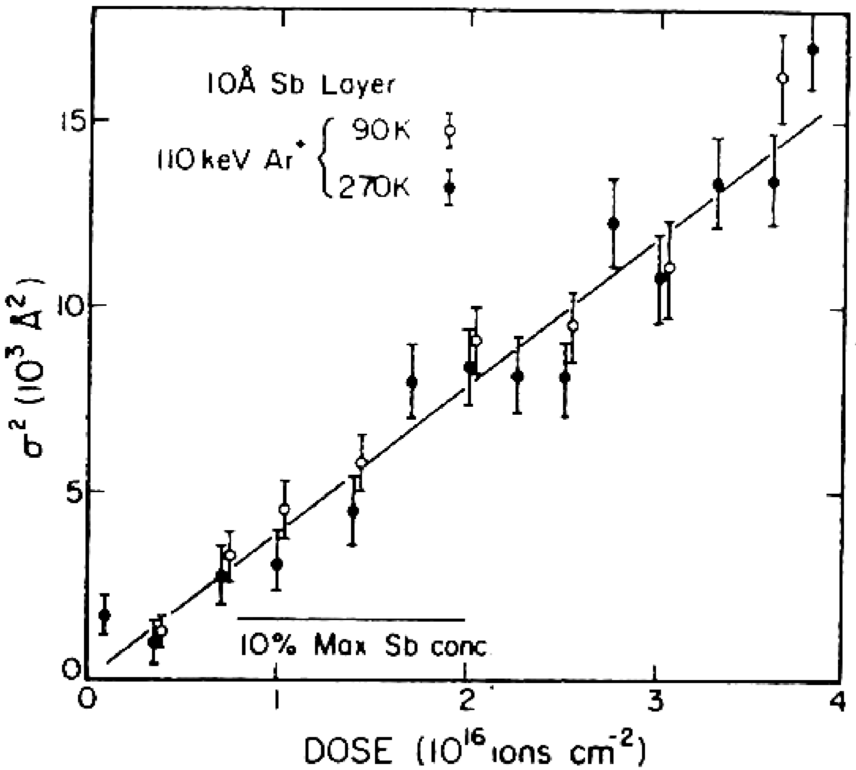

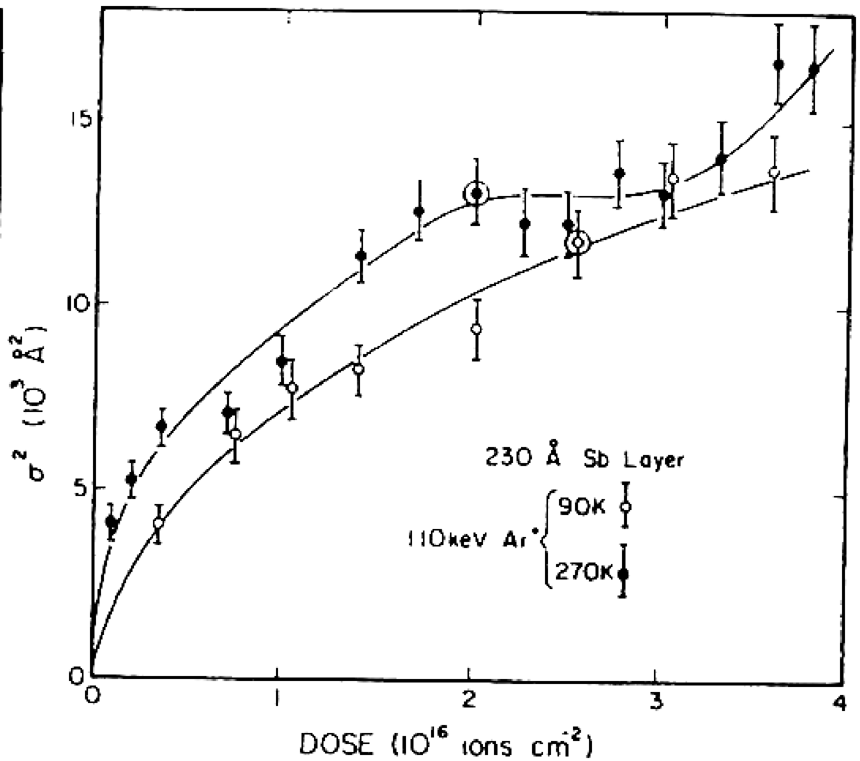

BM Paine et al., MRS Proc., 1982.

RBS on a NIST standard

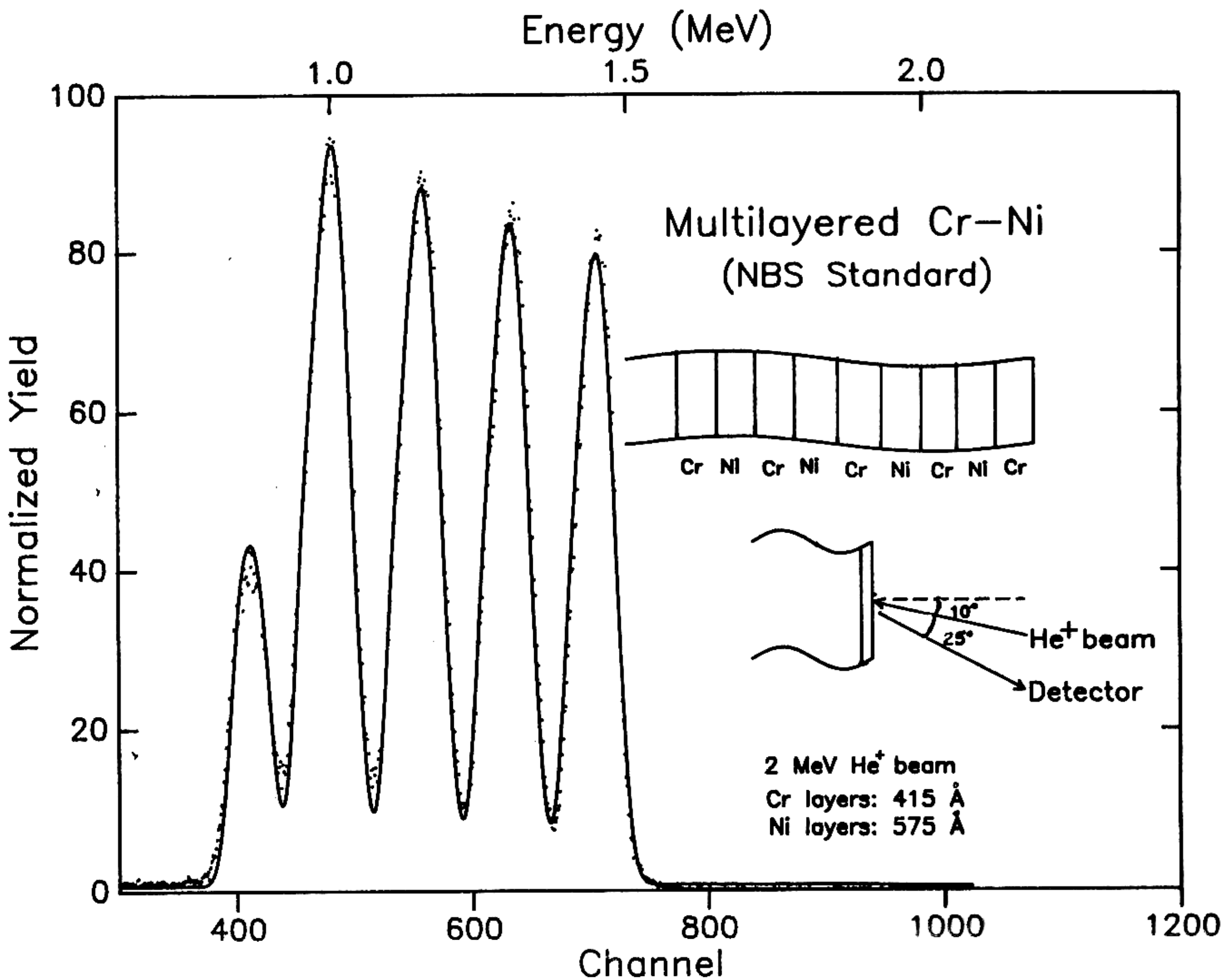

RBS of Mo/$MoSi_2$ multilayers

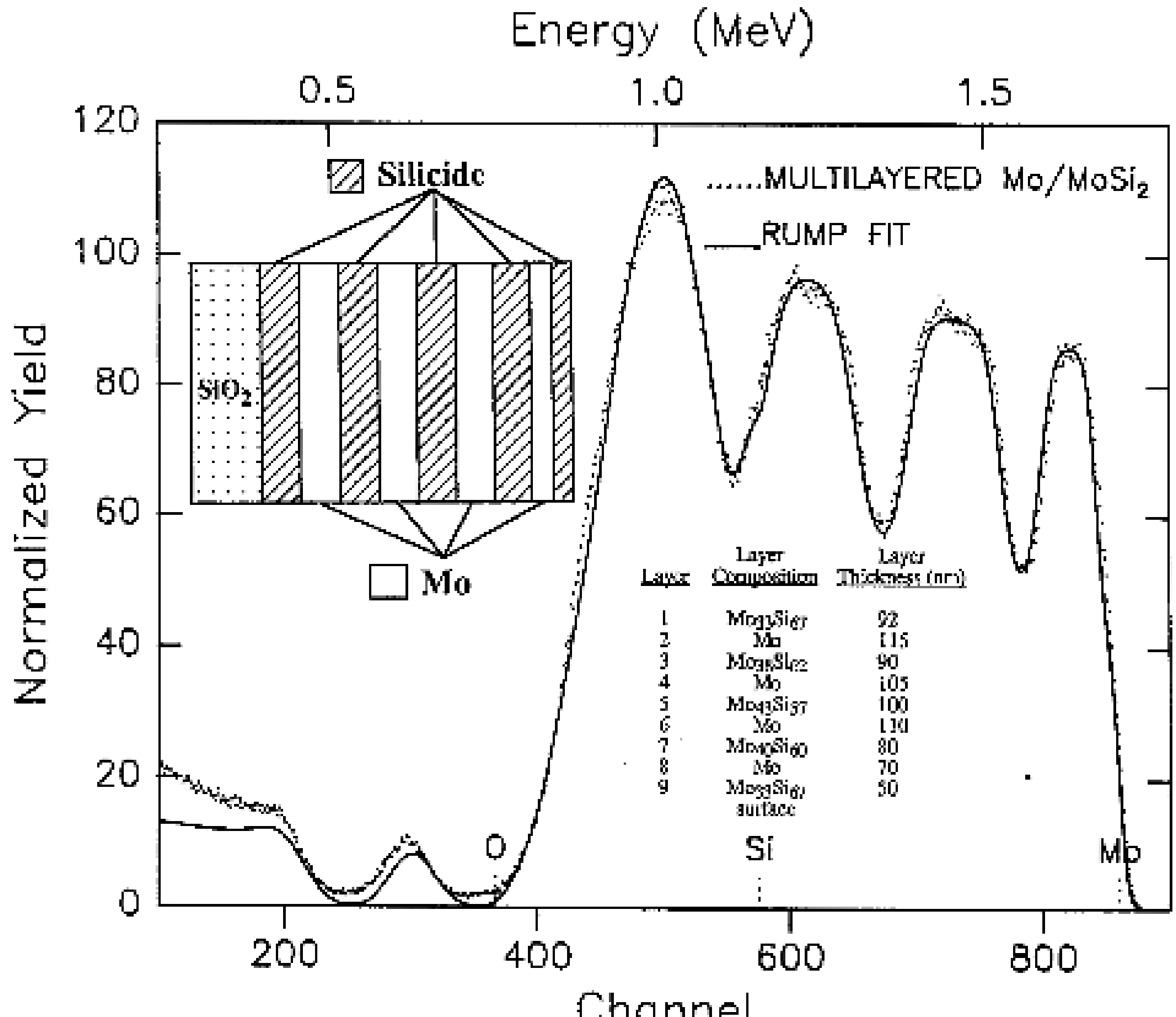

RBS plot of Ag/Cu multilayer 10 nm layer thickness

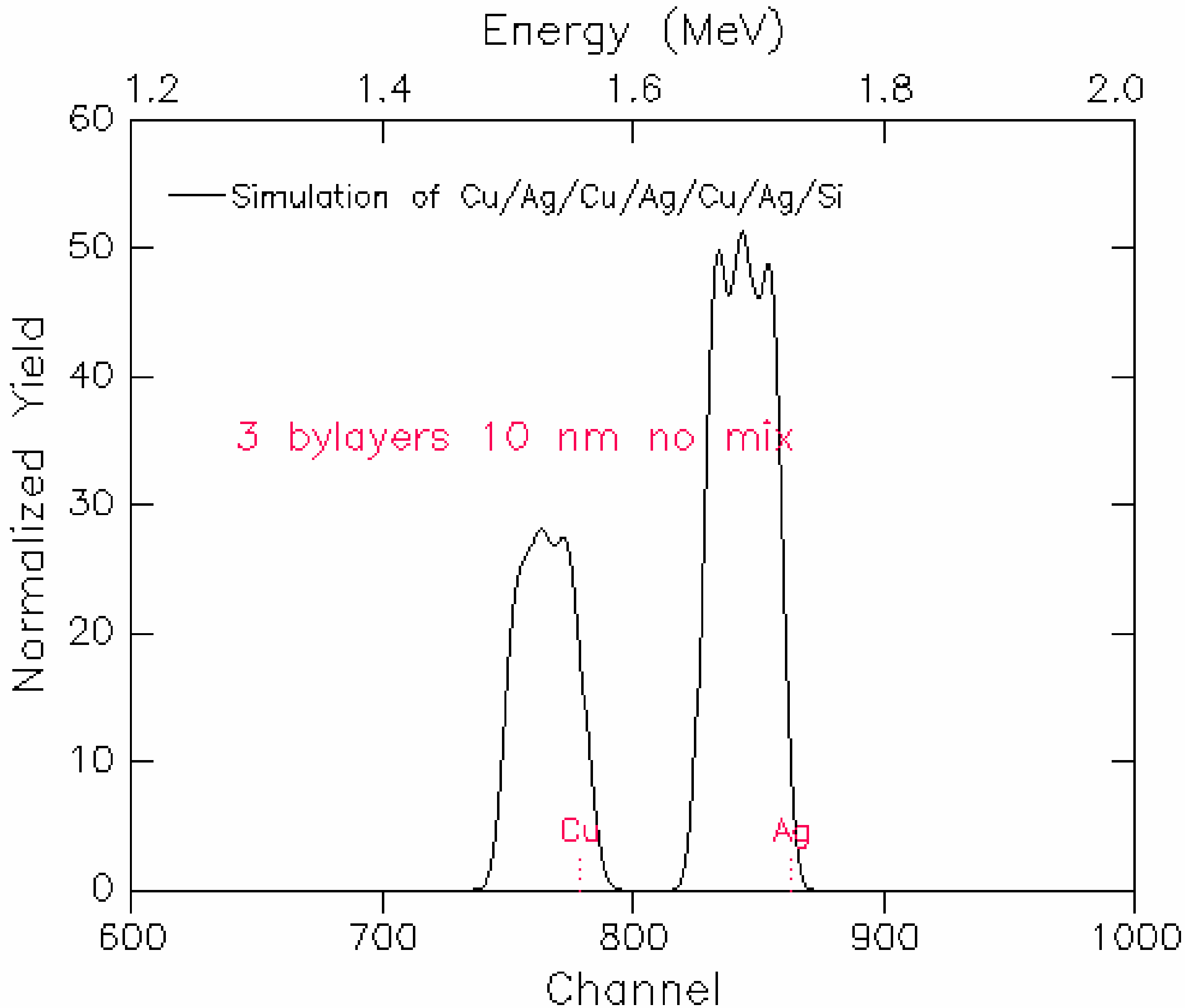

MichiganEngineering

Low temperature ion mixing for several "collisionally similar" bilayer systems

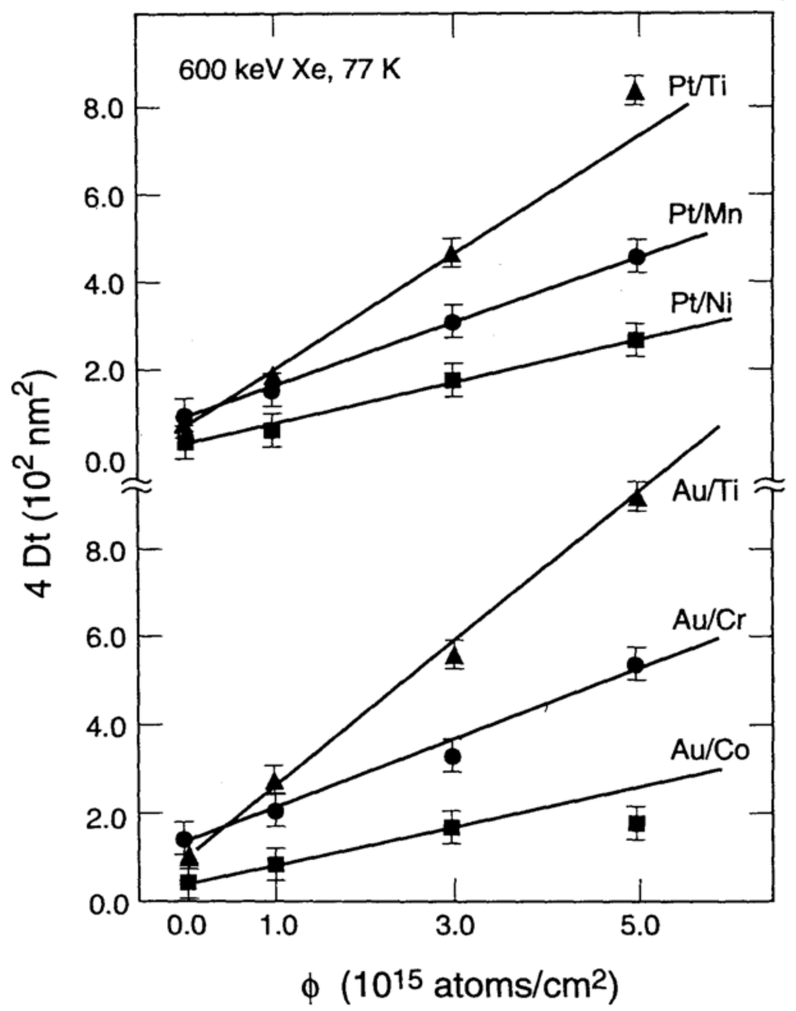

Cheng et al. Appl. Phys.Lett 45 (1984) 185.

The reason is that fundamentally, diffusion is driven by a *chemical potential gradient*, $\nabla\mu(x)$. For non-ideal solutions, we must relate $\nabla\mu(x)$ to $\nabla C(x)$. This is done by replacing D with a modified D' that accounts for the Kirkendall effect and describes diffusional intermixing.

$$D' = [D_A^o C_B + D_B^o C_A]\,[1 + \partial \ln \gamma(C_A) / \partial \ln C_A]$$

$$= D[1 - 2\Delta H_{mix}/k_B T]$$

This eqn. states that random walk will be *biased* when the potential energy depends on the configuration. So mixing rates depend on the degree of Darkin biasing.

Using using this eqn., the effective temperature at which diffusion occurs can be determined to be ~1-2 eV, which also means that this is the particle kinetic energy at which mixing occurs.

MichiganEngineering

Mixing rates and ΔH_{mix} for several metallic bilayer systems irradiated with 600 keV Xe at 77K

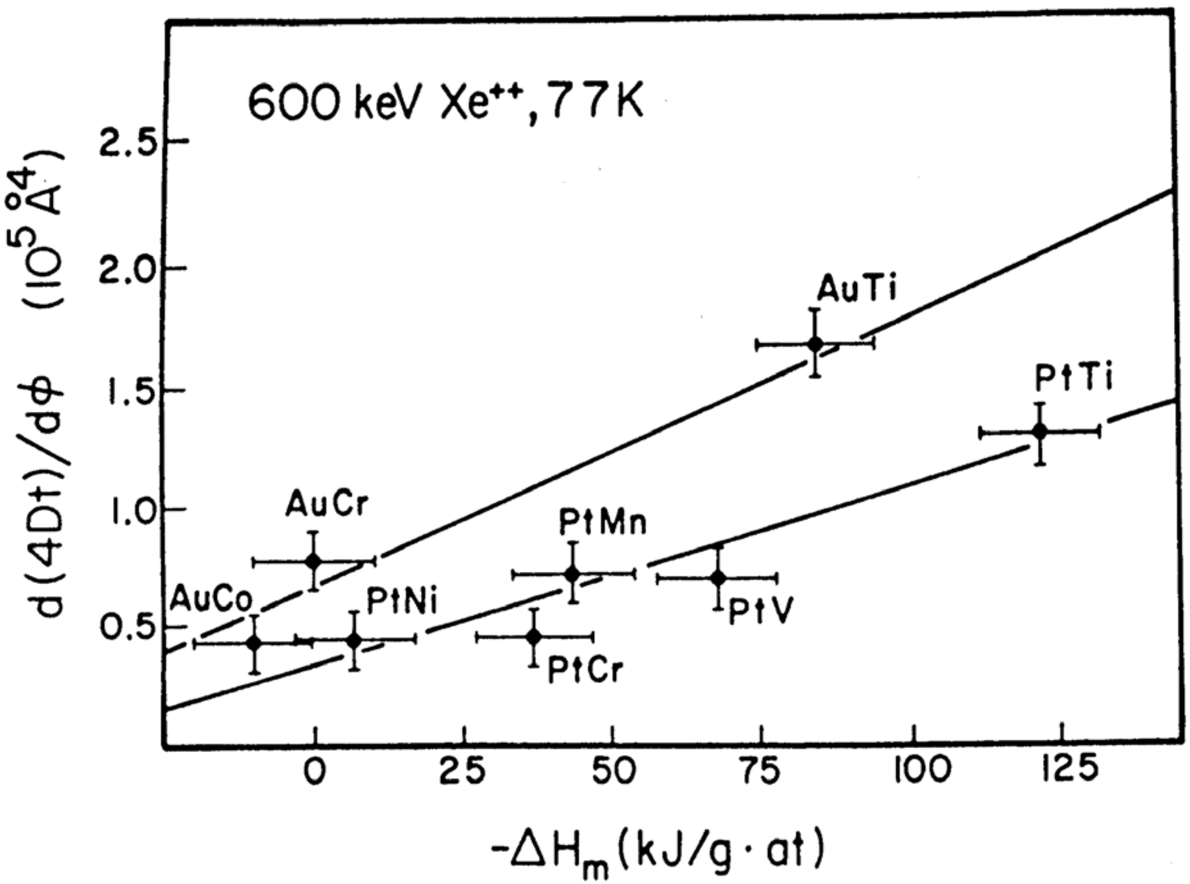

Cheng et al. Appl. Phys. Lett. 45 (1984) 185.

Since mixing depends on the thermodynamic properties, it should depend on ΔH_{COH}, a measure of how tightly bound atoms are in a solid.

The atom jump rate in a thermal spike can be determined from the cascade energy density and used to derive the mixing rate:

$$\frac{d(4Dt)}{d\phi} = \frac{K_1 \varepsilon^2}{N^{5/3}(\Delta H_{COH})^2} \left(1 + K_2 \Delta H_m / \Delta H_{COH}\right)$$

Influence of the cohesive energy on ion mixing

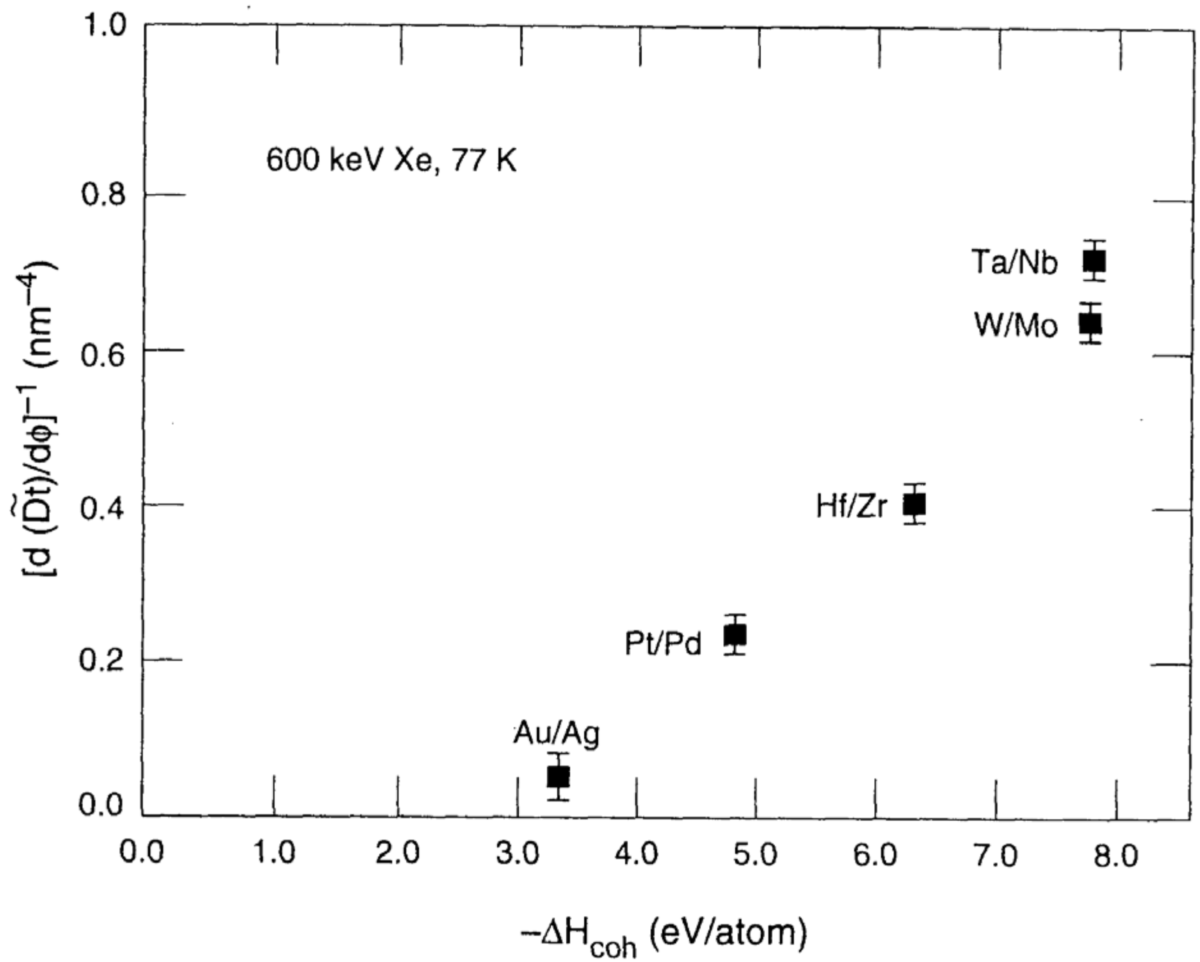

Van Rossum et al. appl. Phys. Lett. 46 (1985) 610.

Experimental mixing data showing a linear relationship between the mixing rate and the ratio $\Delta H_{mix}/\Delta H_{coh}$

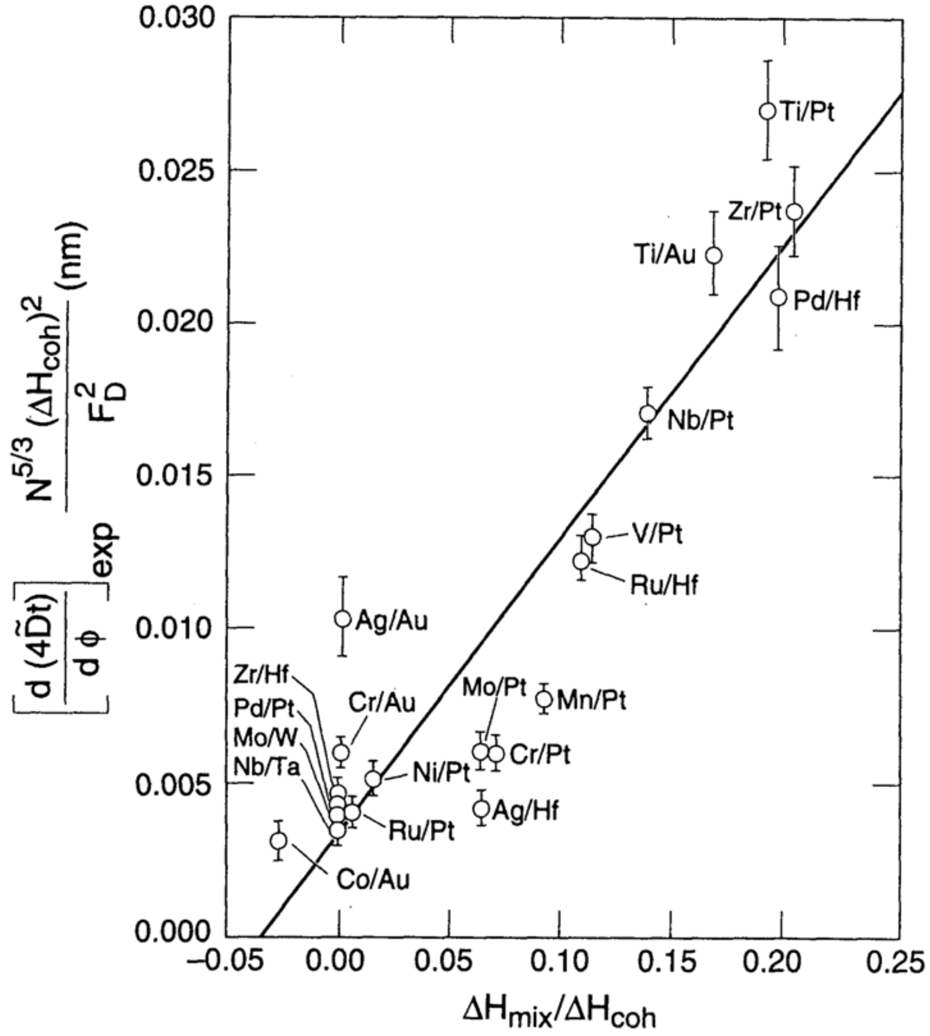

Workman et al., Appl. Phys. Lett. 50 (1087) 1485.

Experimental and calculated ion mixing data for several systems

System (A–B)	$-\Delta H_{mix}$ (kJ/gram-atom)	$-\Delta H_{coh}$ (eV/atom)	F_D (10^3 eV/nm)	$\bar{N}$ (nm^{-3})	$(4\tilde{D}t/\phi)_{exp}$ (nm^4)	$(4\tilde{D}t/\phi)_{calc}$ (nm^4)
Pt/Ti	122	6.60	445	61.4	12.8	10.7
Pt/V	68	6.27	491	69.2	6.8	7.8
Pt/Mn	43	4.82	531	74.0	7.3	11.9
Pt/Cr	36	5.34	530	74.7	4.5	7.8
Pt/Ni	7	5.21	582	78.8	4.5	4.4
Au/Ti	84	5.20	414	57.8	16.3	14.8
Au/Cr	0	3.96	498	71.2	7.8	4.8
Au/Co	−11	3.99	539	74.3	4.5	1.2
Pt/Pd	0	4.87	554	67.1	4.5	4.3
Hf/Zr	0	6.34	355	44.0	2.6	2.2
W/Mo	0	7.86	519	63.6	1.6	1.6
Ta/Nb	0	7.84	445	55.6	1.4	1.5
Au/Ag	0	3.38	480	58.8	23.7	8.4

WL Johnson, et al, Nucl. Instr. Meth B7/8 (1985) 657.

Effect of Temperature

When the temperature increases, we begin to see effects due to radiation-enhanced diffusion and radiation-induced segregation.

Systems with negative heats of mixing will likely mix easily and form intermetallic phases.

Systems with positive heats of mixing will likely resist mixing and will tend to maintain the multilayer structure. Ballistic intermixing will be opposed by thermodynamically-driven demixing and the resulting composition profiles will be a result of these opposing processes.

Dose dependence of ion beam mixing for Ni-Si for 280 keV Kr^+ irradiation at several temperatures

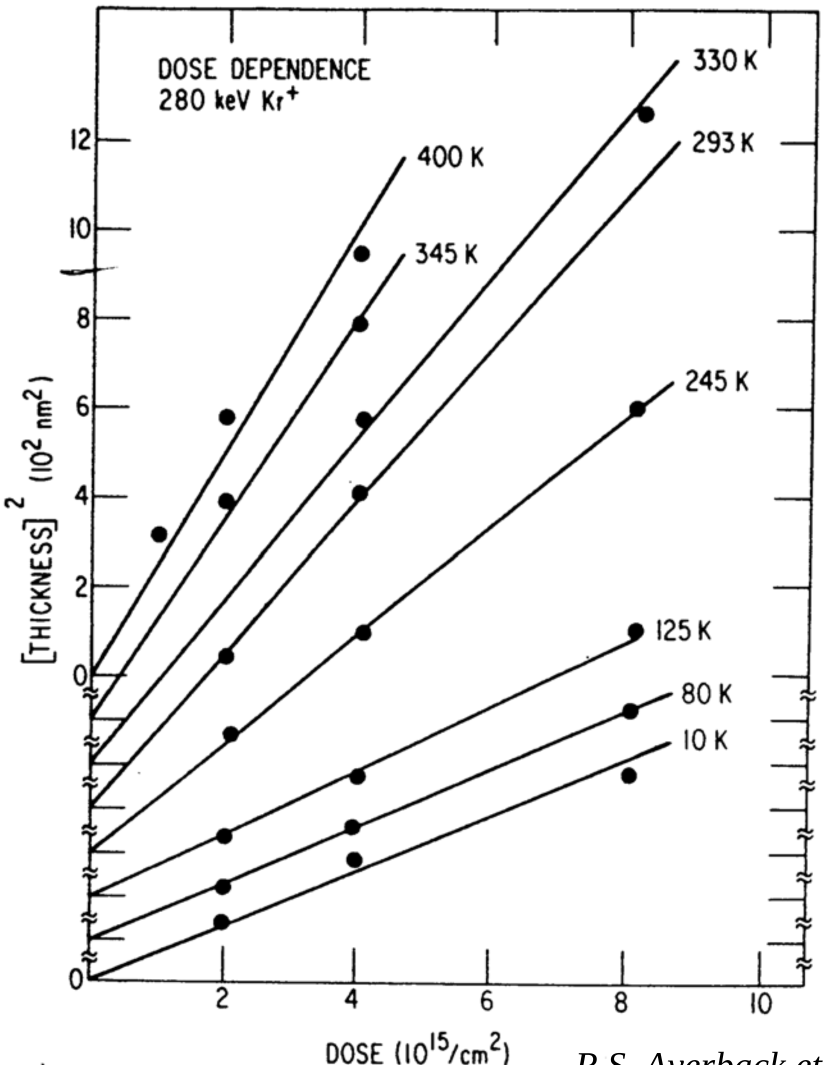

R.S. Averback et al. J. Appl. Phys. 53 (1982) 1342

Influence of temperature on mixing in Al/Mo

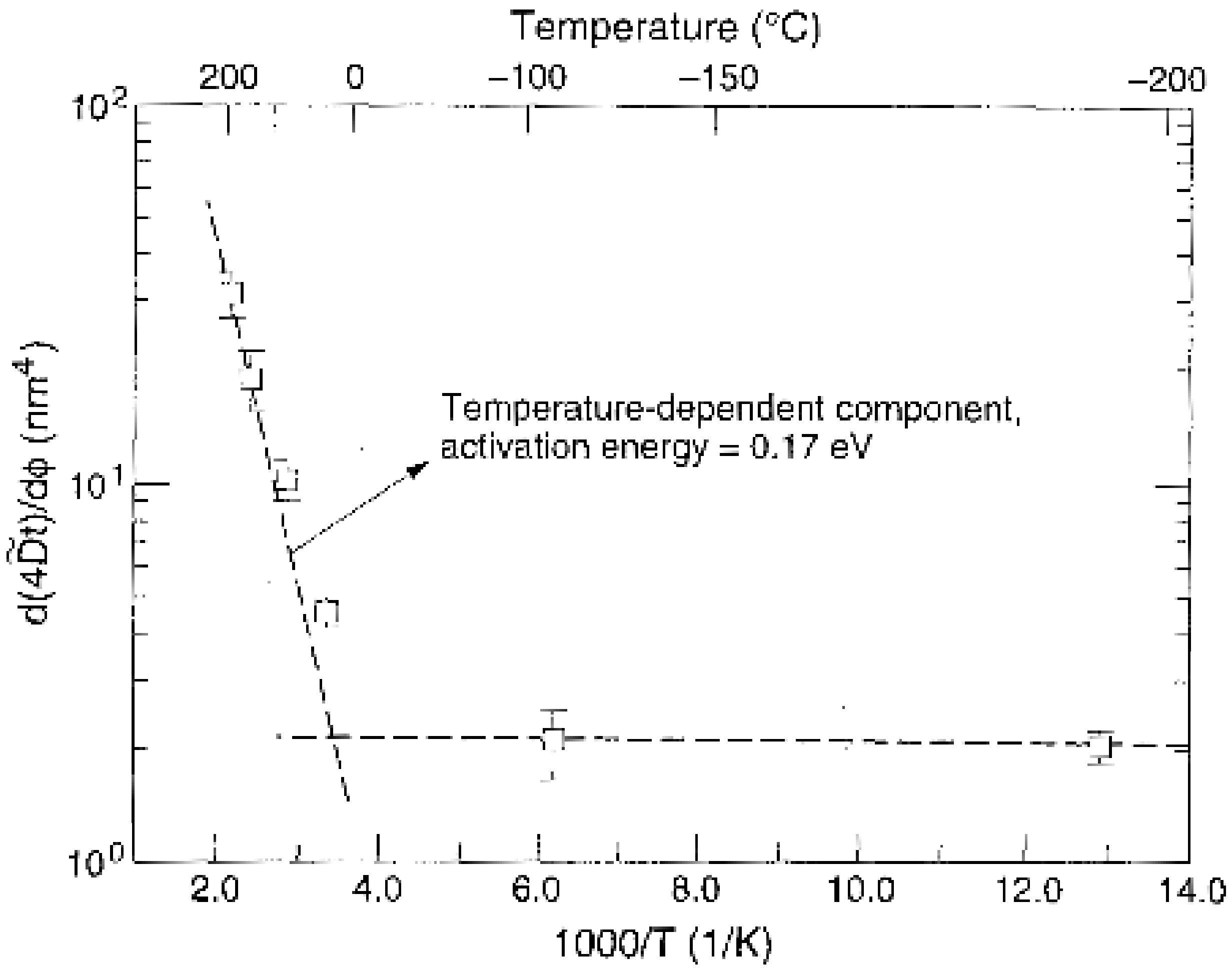

E. Ma, et al., Appl. Phys. Lett. 54 (1989) 413.

Correlation between ballistic mixing (T-independent) and temperature-dependent mixing transition, T_c and the average cohesive energy of the bilayer alloy

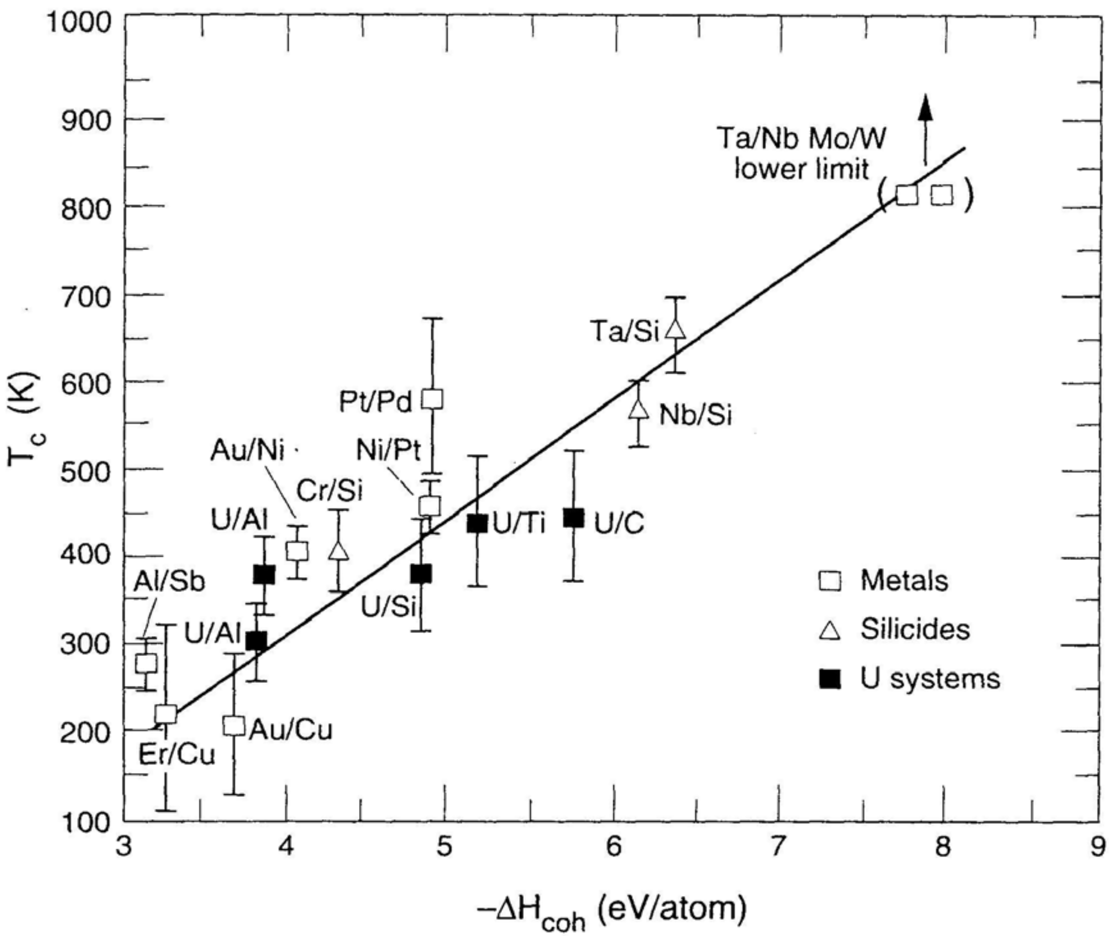

Cheng et al. J. Appl. Phys. 60 (1986) 2615.

Effect of irradiating particle mass and energy

- Light, high energy ions produce large cascade volume but with widely separated spikes and minimal overlap.
- Heavy ions produce a smaller total cascade volume in few spikes that are closely spaced or overlapping.
- Overall, the overlap of heavy ion irradiation results in a higher mixing efficiency for heavy ions.

Formation of γ’-Ni_3Si on defect sinks in a solid-solution Ni-Si alloy due to radiation induced segregation

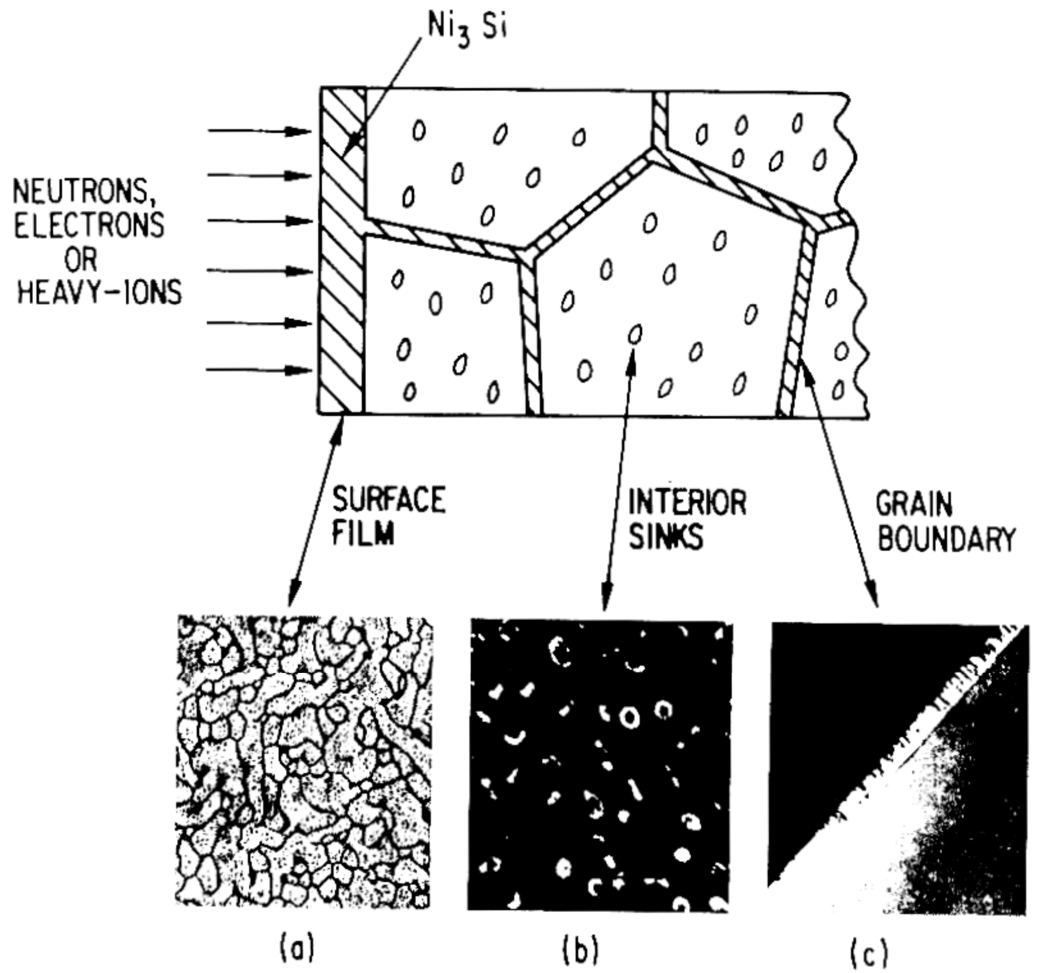

L. E. Rehn, et al., Metastable Materials Formation by Ion Irradiation, Elsevier (1982) 17.

Variation in composition near a grain boundary in Fe-12Cr-15Ni-0.95Si after irradiation to 23.6 dpa at 645°C

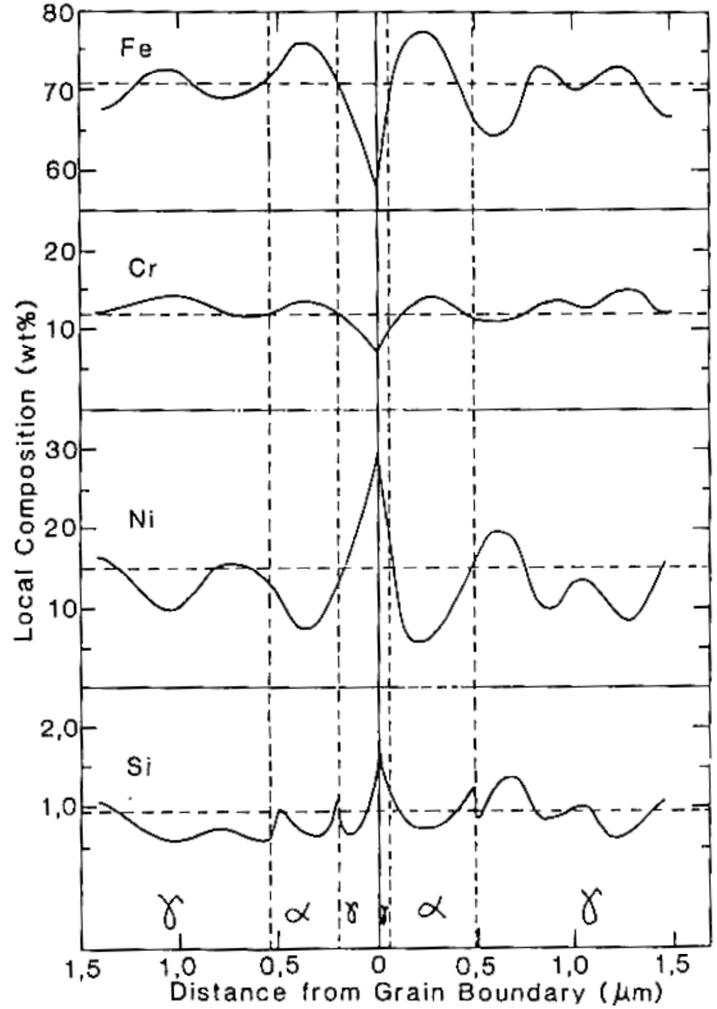

T. M. Williams, et al., Radiation Induced Sensitization of Stainless Steels, Berkeley Nuclear Labs,(1987) 116.

MichiganEngineering

Comparison of γ' in proton- and neutron-irradiated SS

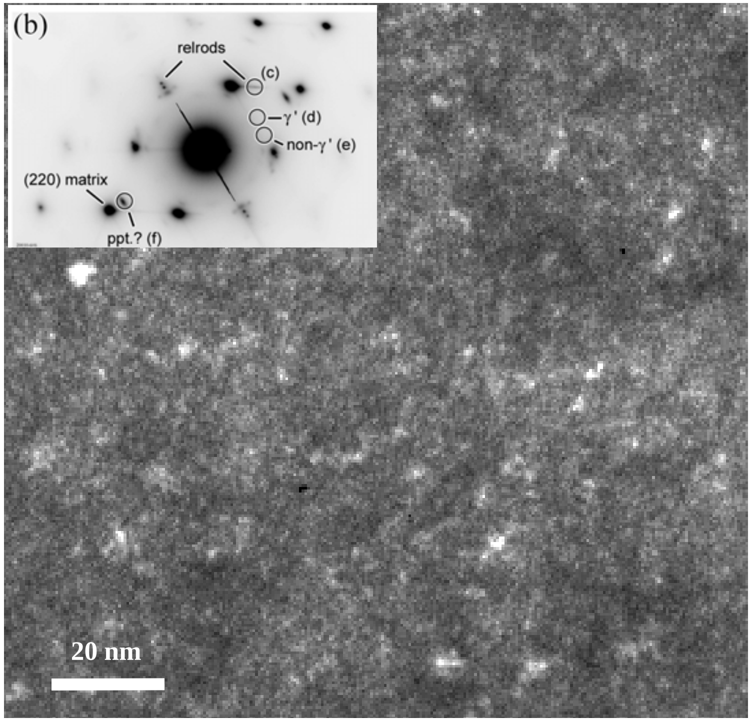

Tihange baffle bolt:
neutron-irradiated to ~7 dpa at 299°C*.

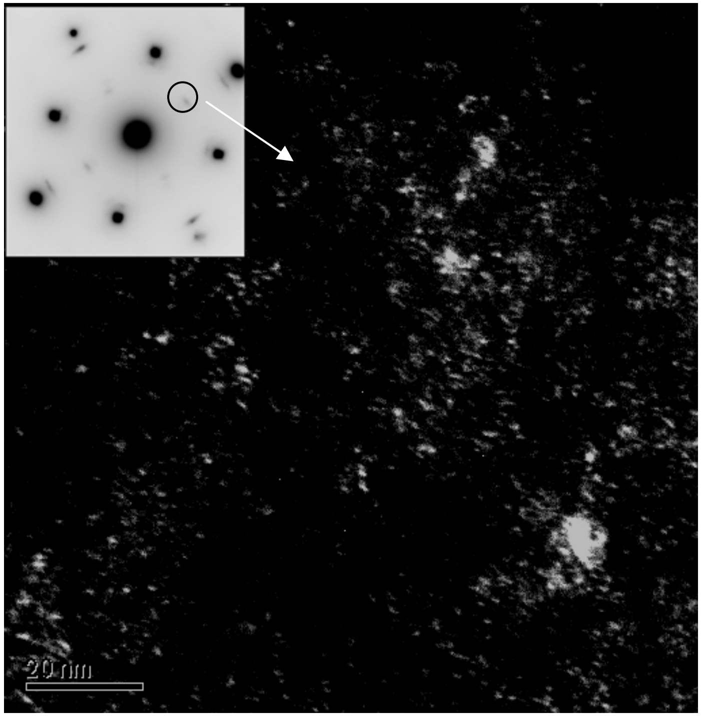

heat H proton-irradiated to 5.5 dpa at 360°C.

•ATEM Characterization of Stress-Corrosion Cracks in LWR-Irradiated Austenitic Stainless Steel Core Components, PNNL EPRI Report, 11/2001.
•Image resized for equivalent scale.

MichiganEngineering

Comparison of precipitation in proton- and neutron-irradiated SS

	Tihange baffle bolt: neutrons 299°C to ~7 dpa*	heat H: protons 360°C to 5.5 dpa
Size	few nm	2.2 nm (0.2 % vol.fraction)
Location	In matrix of grains, Not observed at GB	In matrix of grains, None found at GB
Composition	Ni, Si enriched Cr depleted	Significant Ni, Si enrichment Cr depletion

Extra spot is not gamma prime

* *ATEM Characterization of Stress-Corrosion Cracks in LWR-Irradiated Austenitic Stainless Steel Core Components, PNNL EPRI Report, 11/2001.*

Wavelength of compositional fluctuation in neutron-irradiated SS

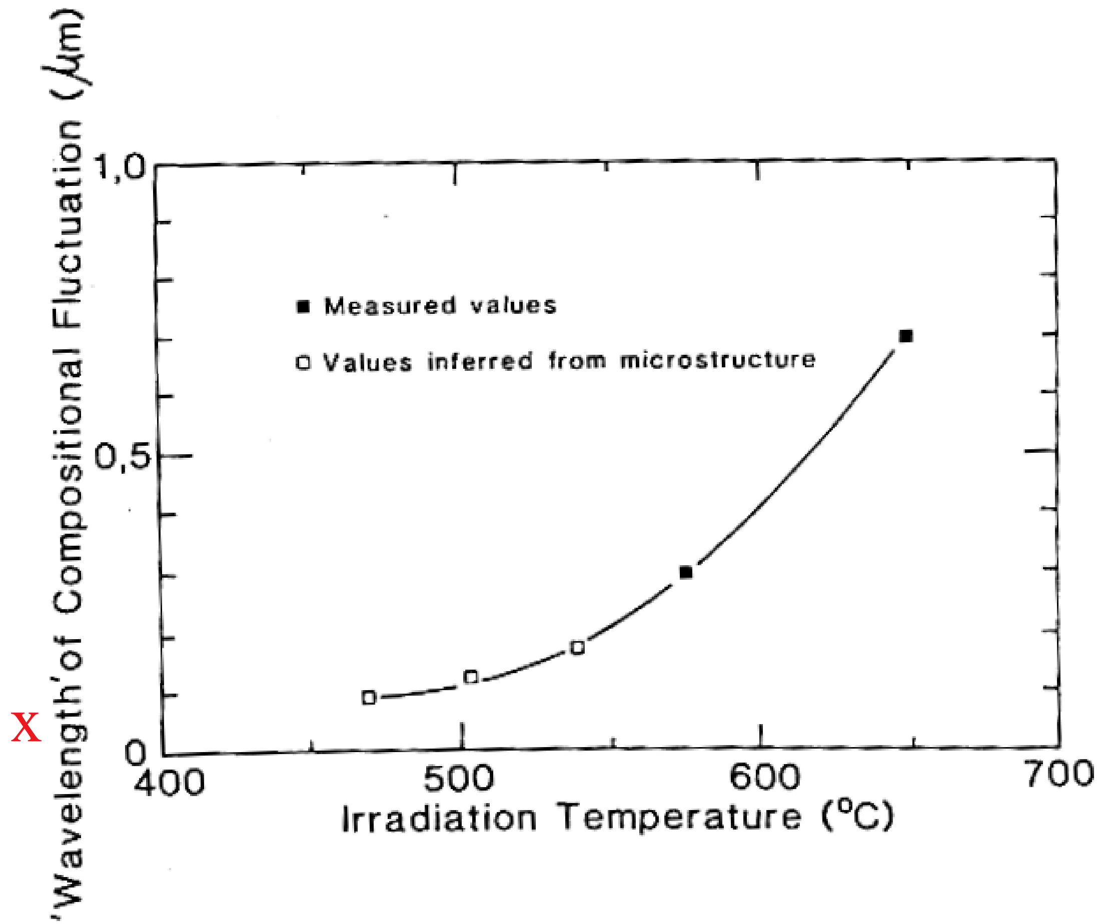

Irradiation of Multilayer Structures

Flux-normalized displacement rate as a function of depth for various particles

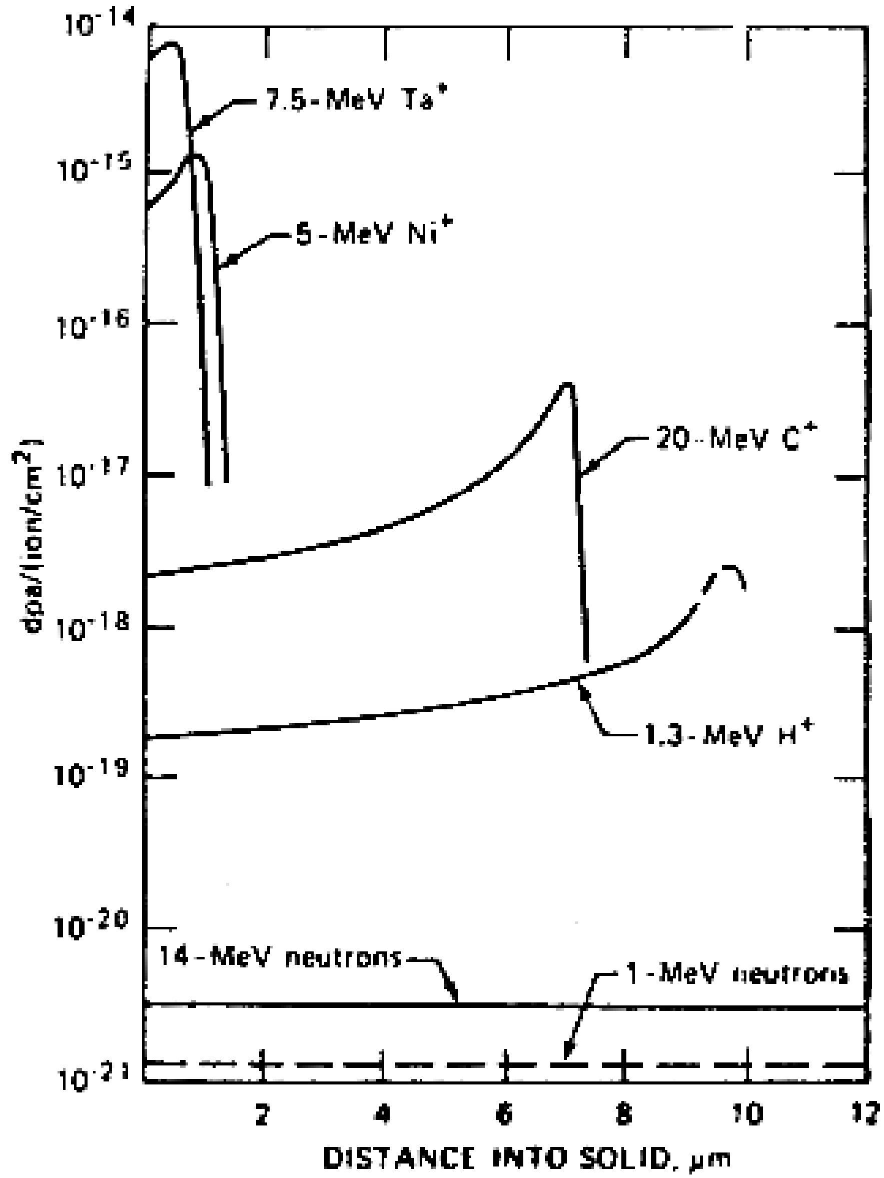

G.L. Kulcinski et al, Radiation-Induced Voids in Metals, 1972

MichiganEngineering

3.2 MeV proton damage profile

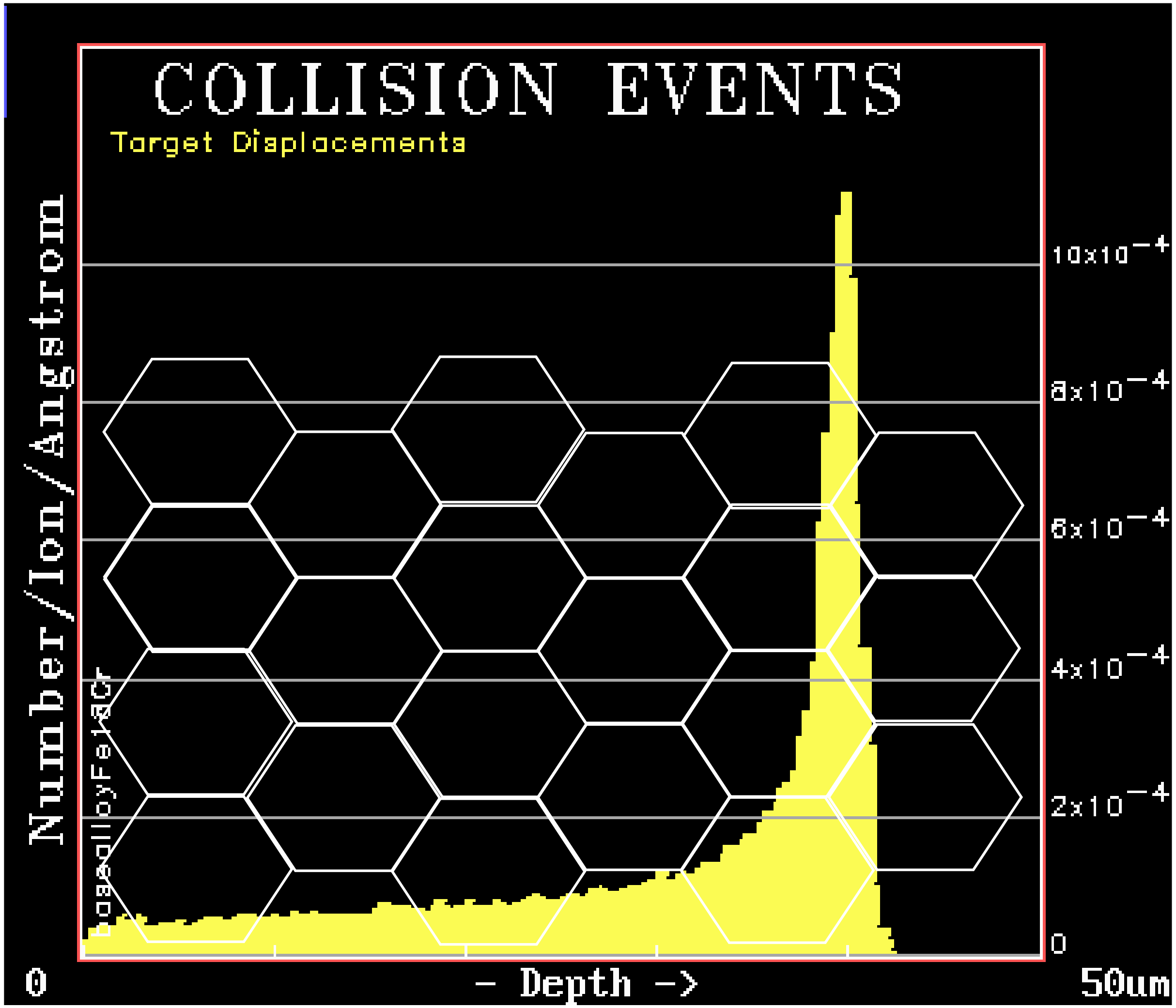

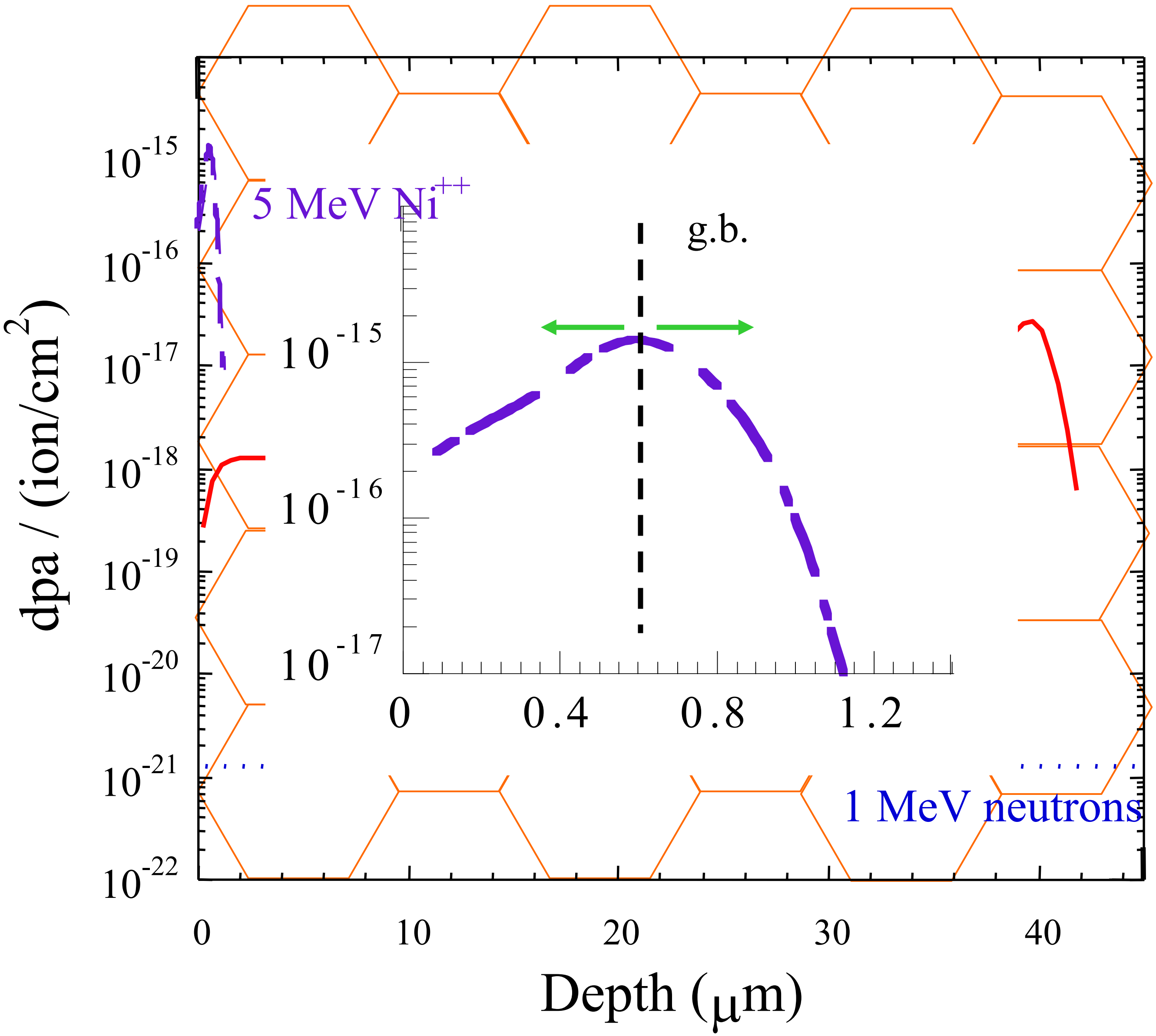

MichiganEngineering

Proton irradiation in the Michigan Ion Beam Laboratory

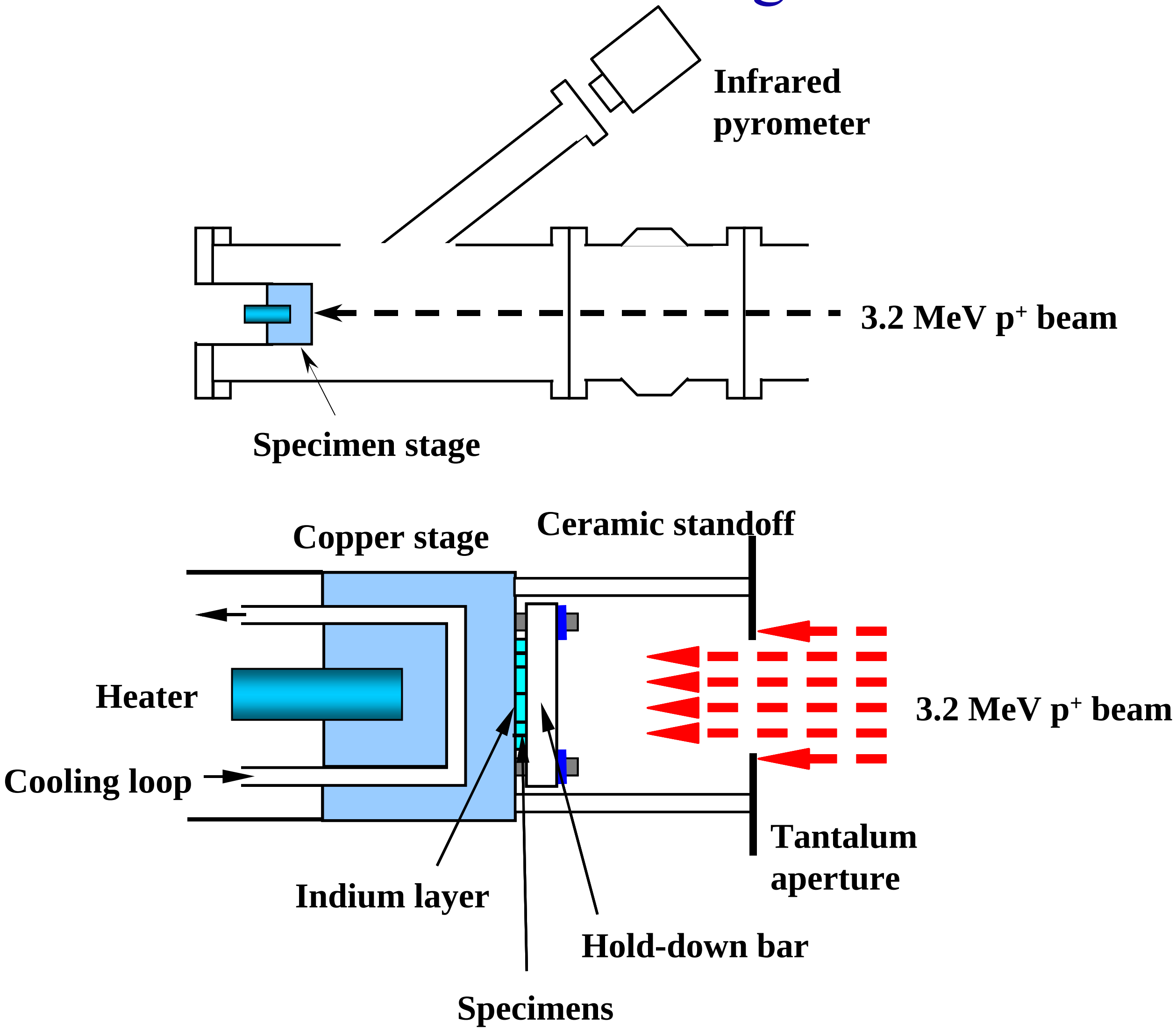

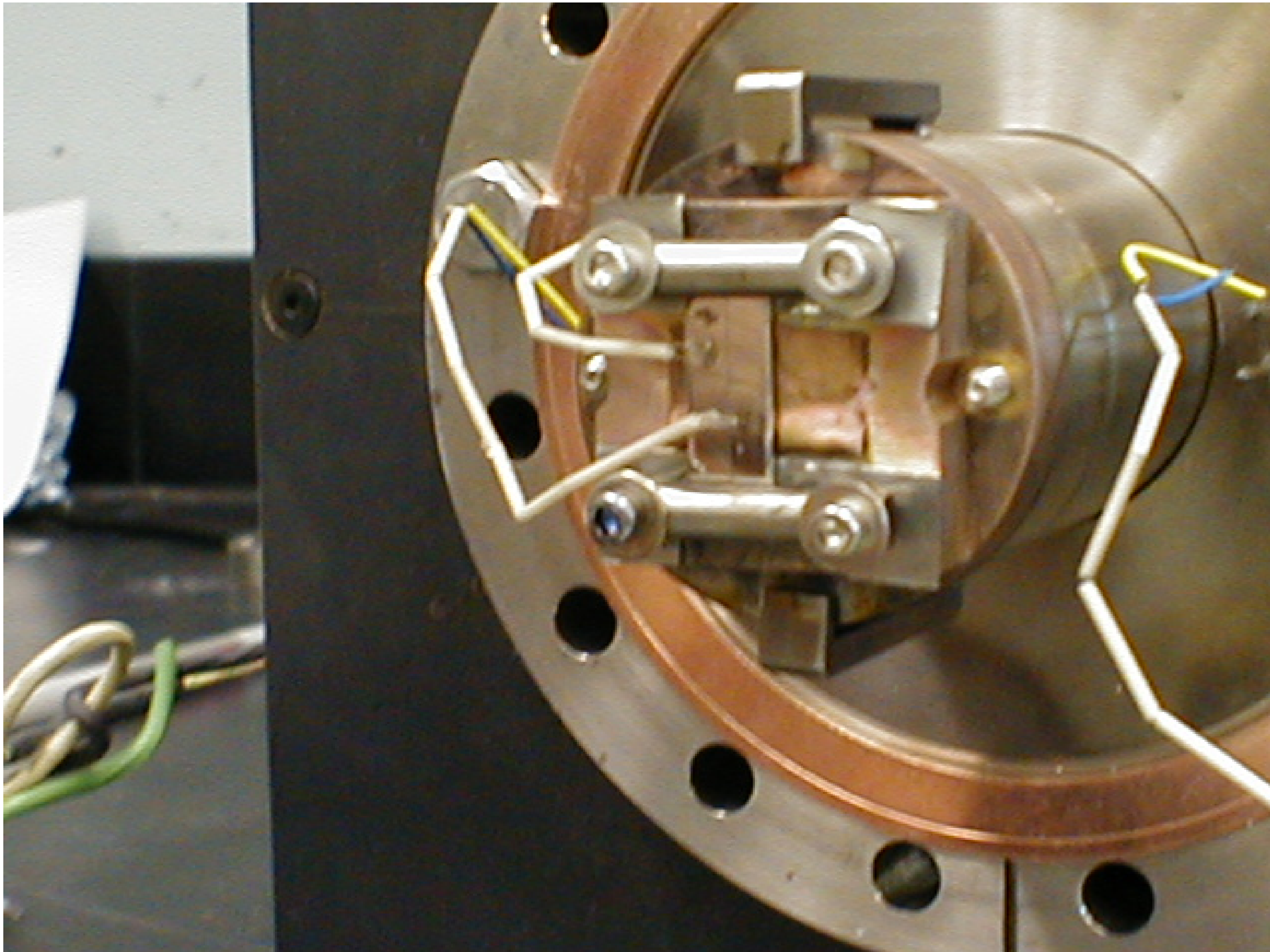

Temperature control during proton irradiation

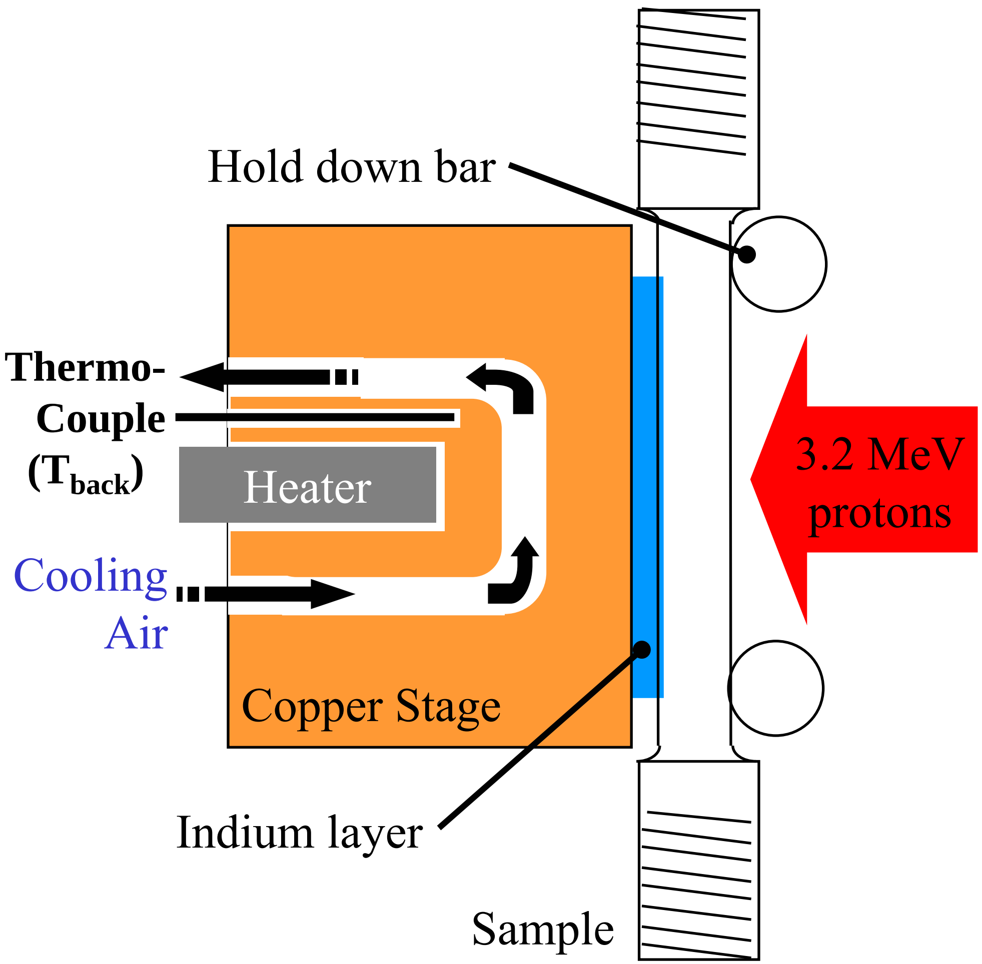

In general,

$$q'' = -k\frac{dT}{dx}$$

or,

$$q'' = k\frac{(T_{surf} - T_{back})}{\Delta x}$$

$$= U_{eff}\ (T_{surf} - T_{back})$$

where,

$$\frac{1}{U_{eff}} = \frac{L_{Cu}}{k_{Cu}} + \frac{L_{In}}{k_{In}} + \frac{L_{SS}}{k_{SS}} + \frac{1}{k_{gap}}$$

Key to Temperature Control

- T_{back} is carefully monitored as beam current is steadily increased until T_{back} approaches 200°C.
- Higher beam currents are possible for higher temperature irradiations (T = 400°C).

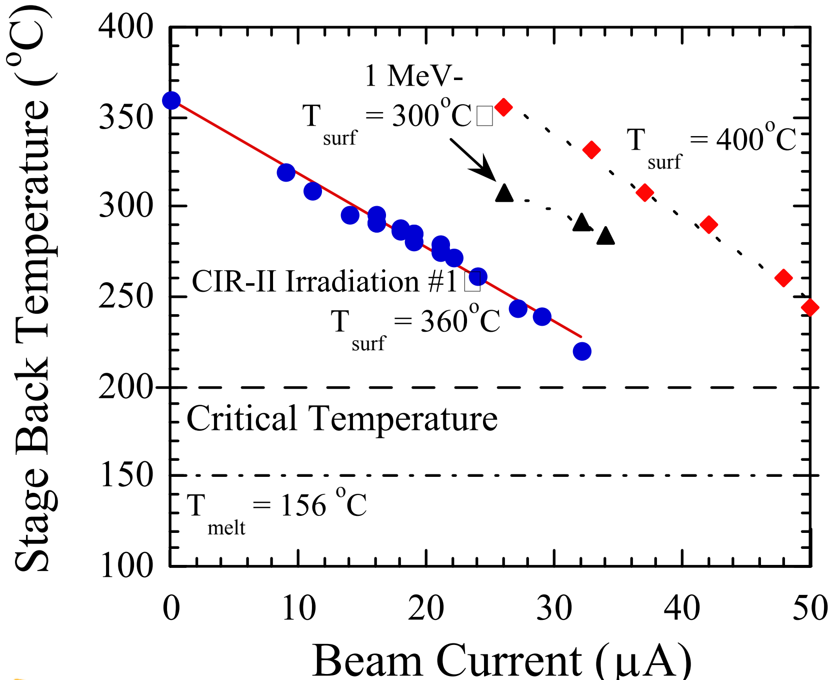

- Critical temperature can be reduced for lower irradiation temperatures (T = 360°C or 300°C) by alloying In and Ga to reduce the melting point of the interface material.

MichiganEngineering

Determination of heat transfer coefficient

- Conductance can be determined from beam current (heat flux) and $T_{back.}$

$$\frac{1}{U_{eff}} = \frac{L_{Cu}}{k_{Cu}} + \frac{L_{In}}{k_{In}} + \frac{L_{SS}}{k_{SS}} + \frac{1}{k_{gap}}$$

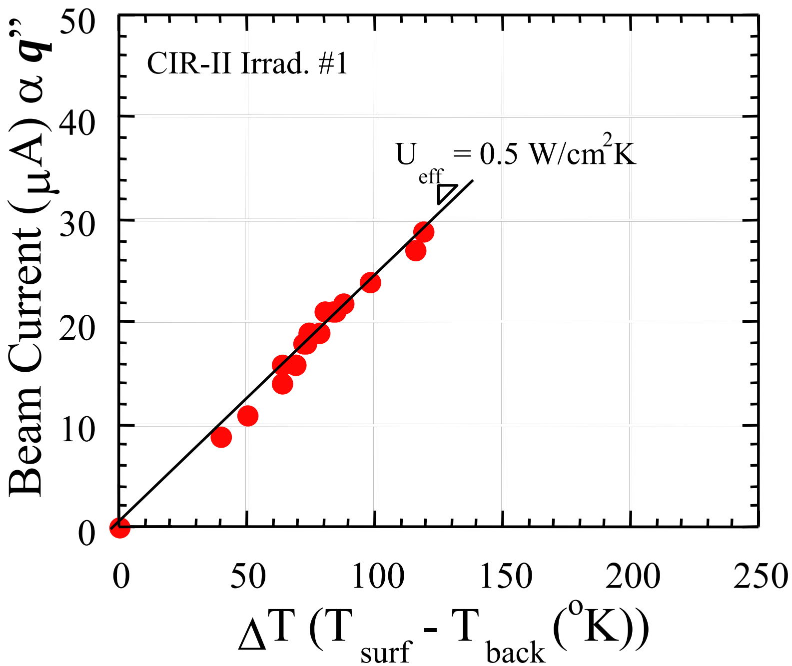

- Experimental conductance is 0.50 W/cm^{2}K.
- Theoretical conductance for existing stage is U_{eff} = 0.69 W/cm^{2}K, with no gap resistance (i.e., perfect interface)

Grain boundary Cr depletion in proton and neutron irradiated stainless steels

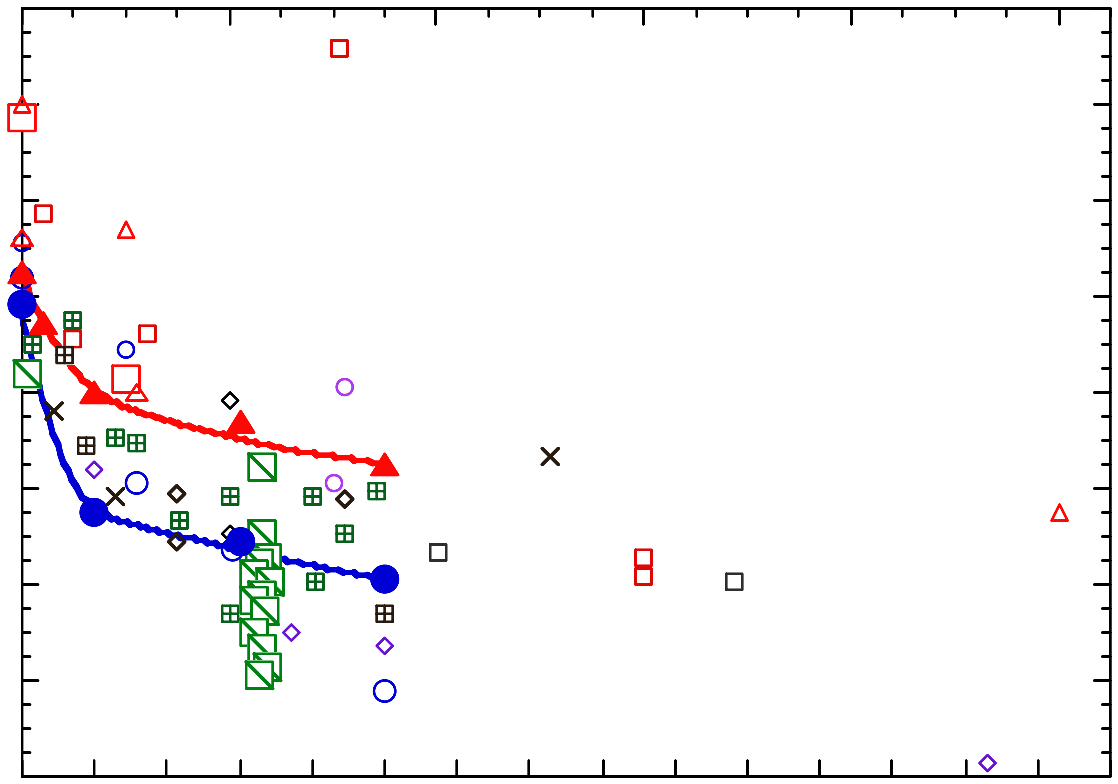

Dose dependence of yield strength as determined from hardness (proton- and neutron-irradiated) and shear punch (neutron-irradiated) measurements

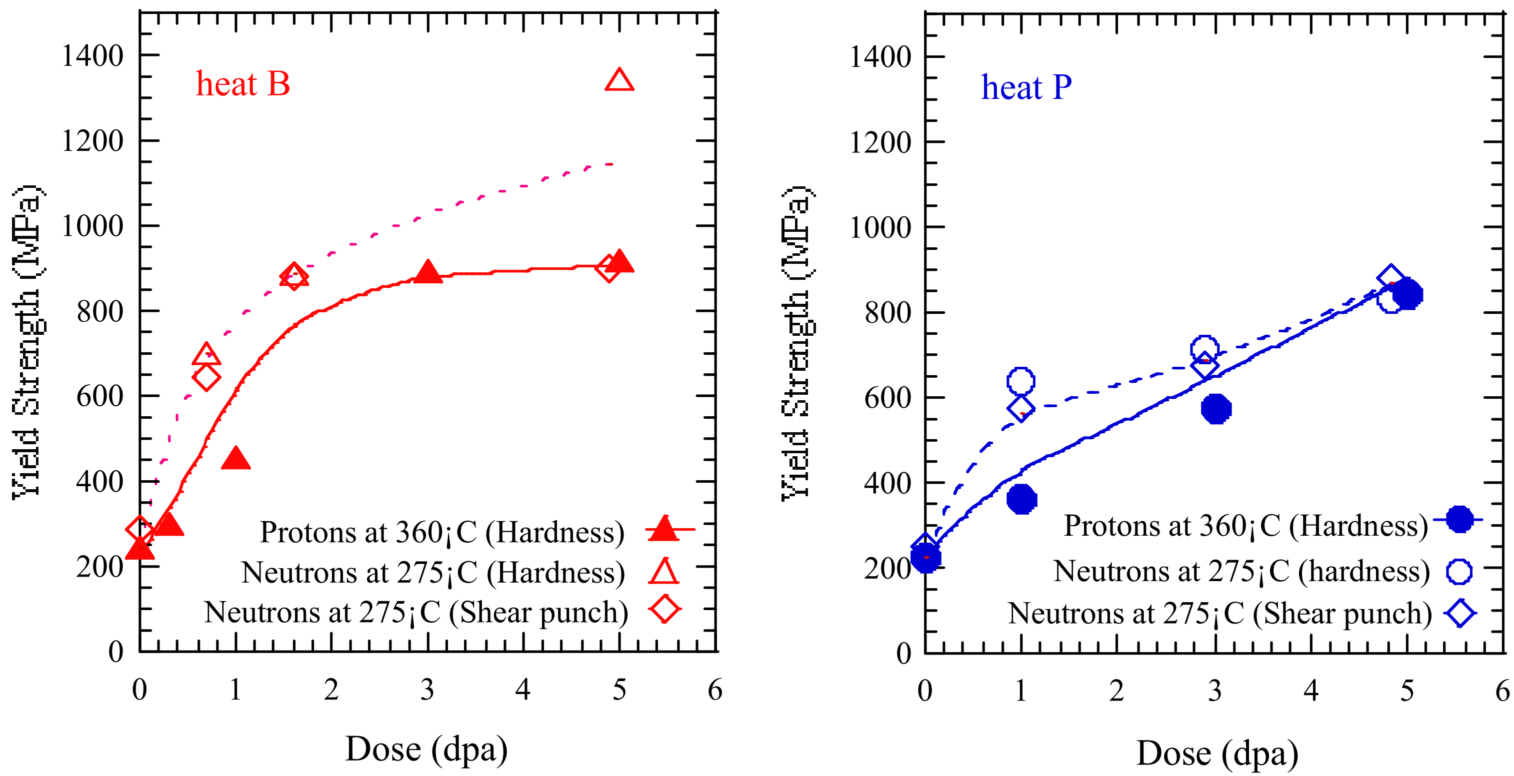

MichiganEngineering

Proton-neutron comparison: IGSCC susceptibility in NWC of 304 SS

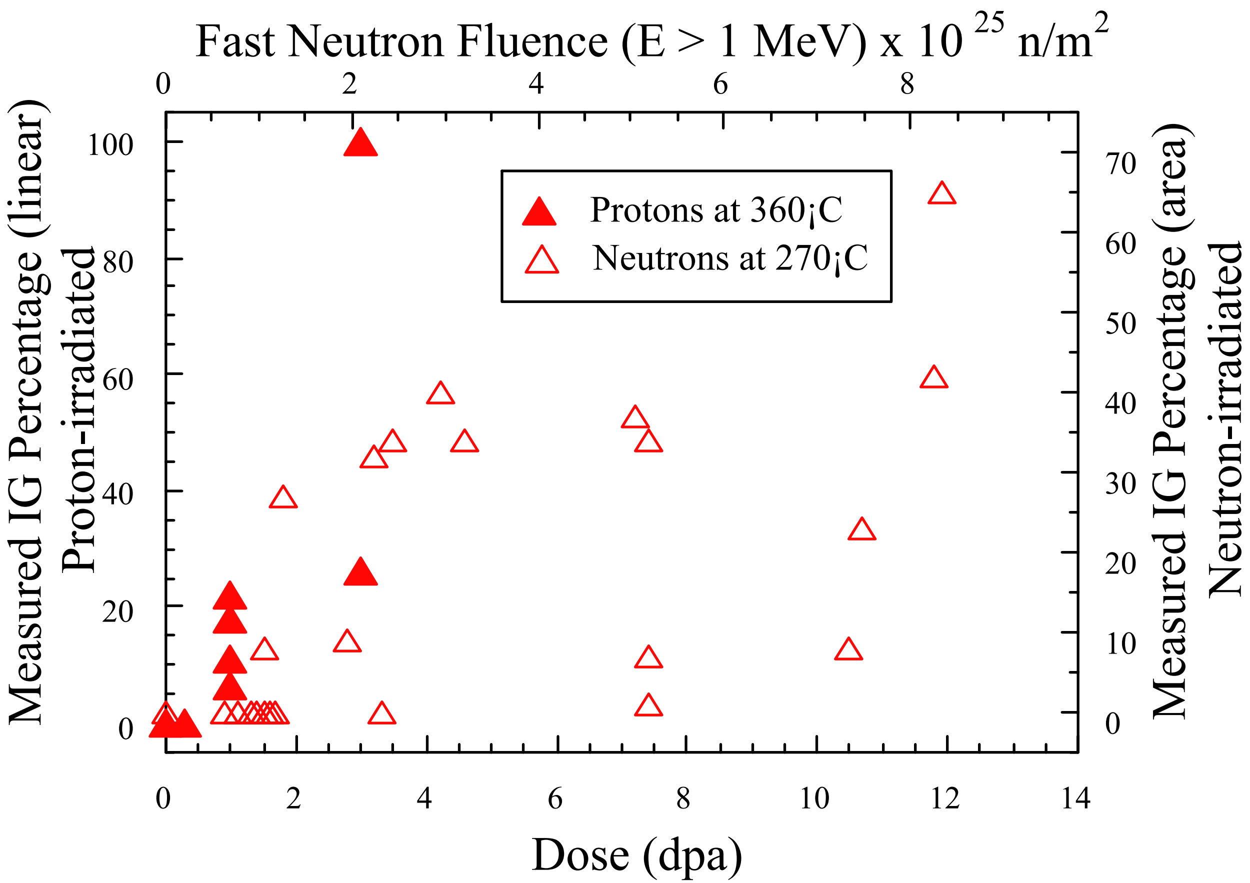

%IG area measurements made by ABB (taken from CIR database)
Proton-irradiated samples strained to failure.
Neutron-irradiated samples strained for 168 hours.

MichiganEngineering

Yield stress increase vs. dose for model RPV steels

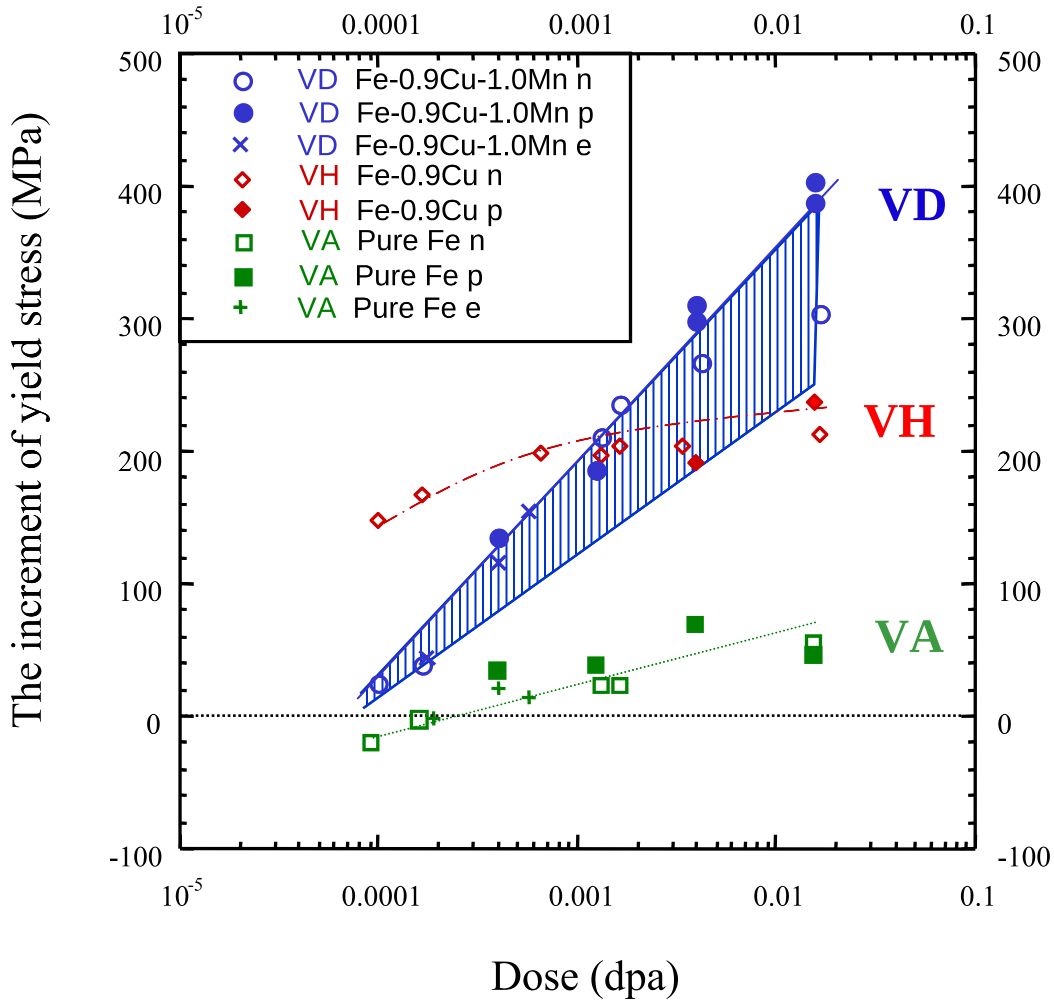

T=300°C

p: 3 x10^{-7}dpa/s

e: 7 x10^{-9}dpa/s

n: 3 x10^{-10}dpa/s

Radiation hardening of proton and neutron irradiated Zircaloy alloys

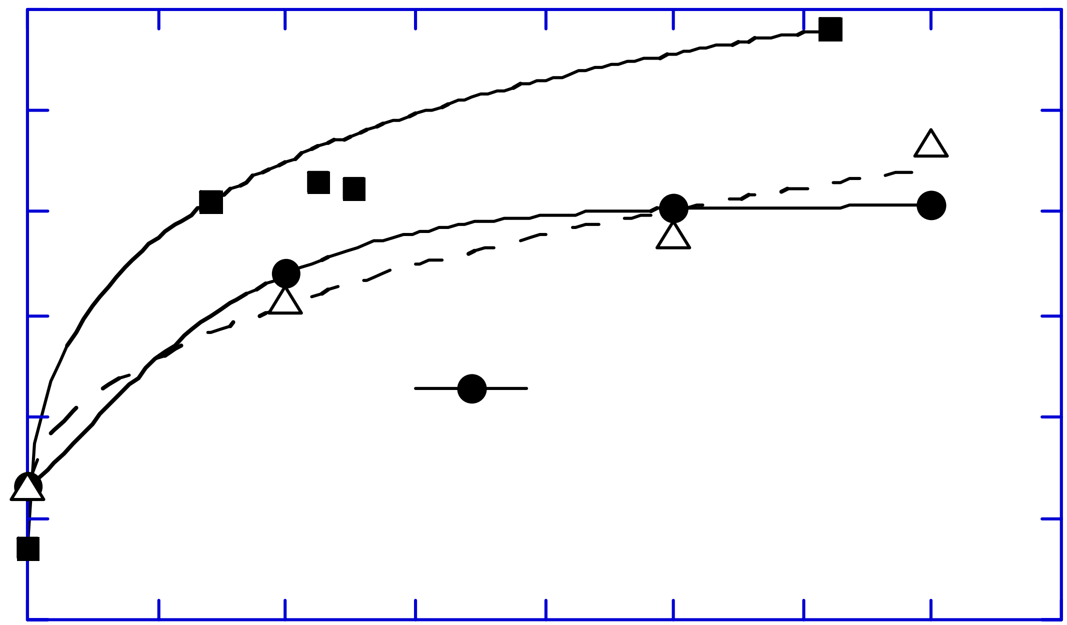

Schematic of PNNL ion irradiation stage (J. Gan, 7-23-2002)

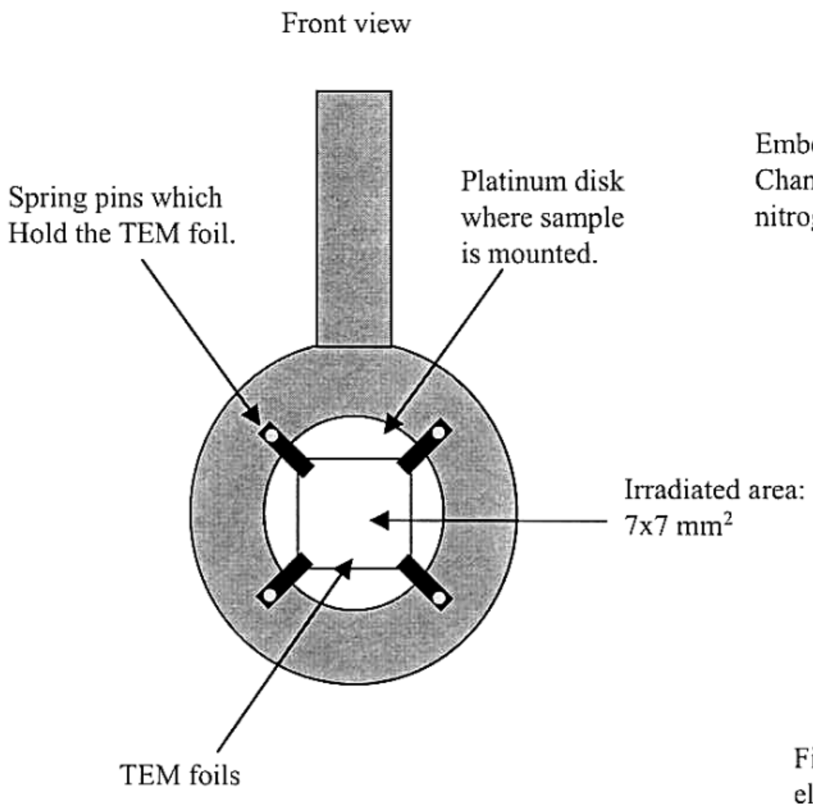

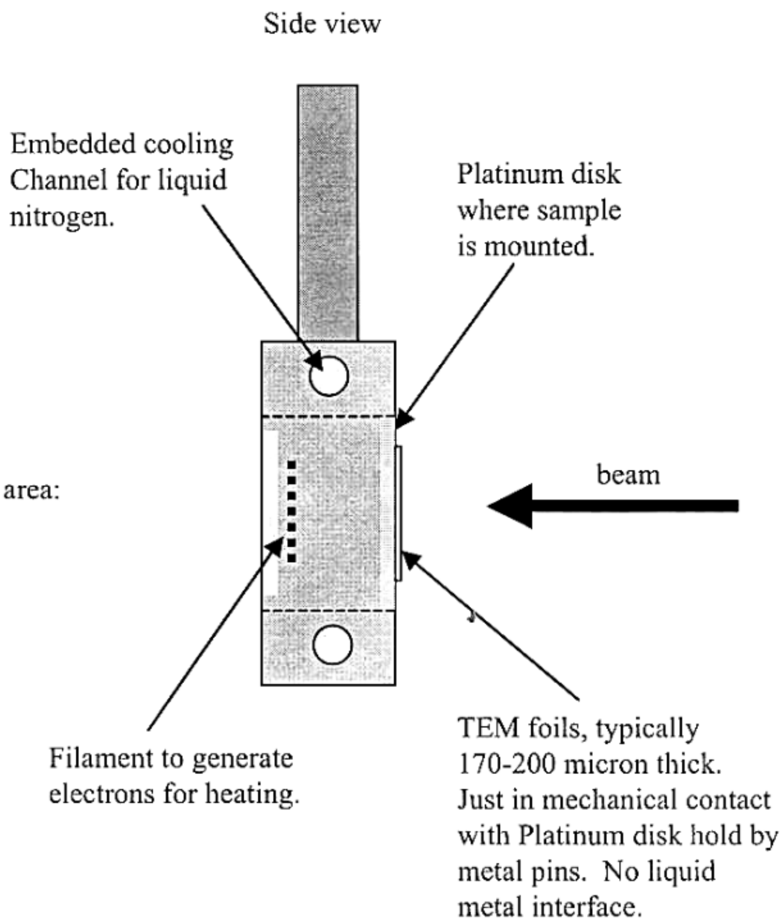

Between filament and platinum disk there is about keV potential to accelerate electrons to bombard the platinum disk, this is the way to heat the stage where the TEM foil sits. Cooling is achieved by running liquid nitrogen through cooling channel at a fixed rate. Temperature control is achieved through control of filment current and electron accelerating voltage.

ORNL Irradiation Stage

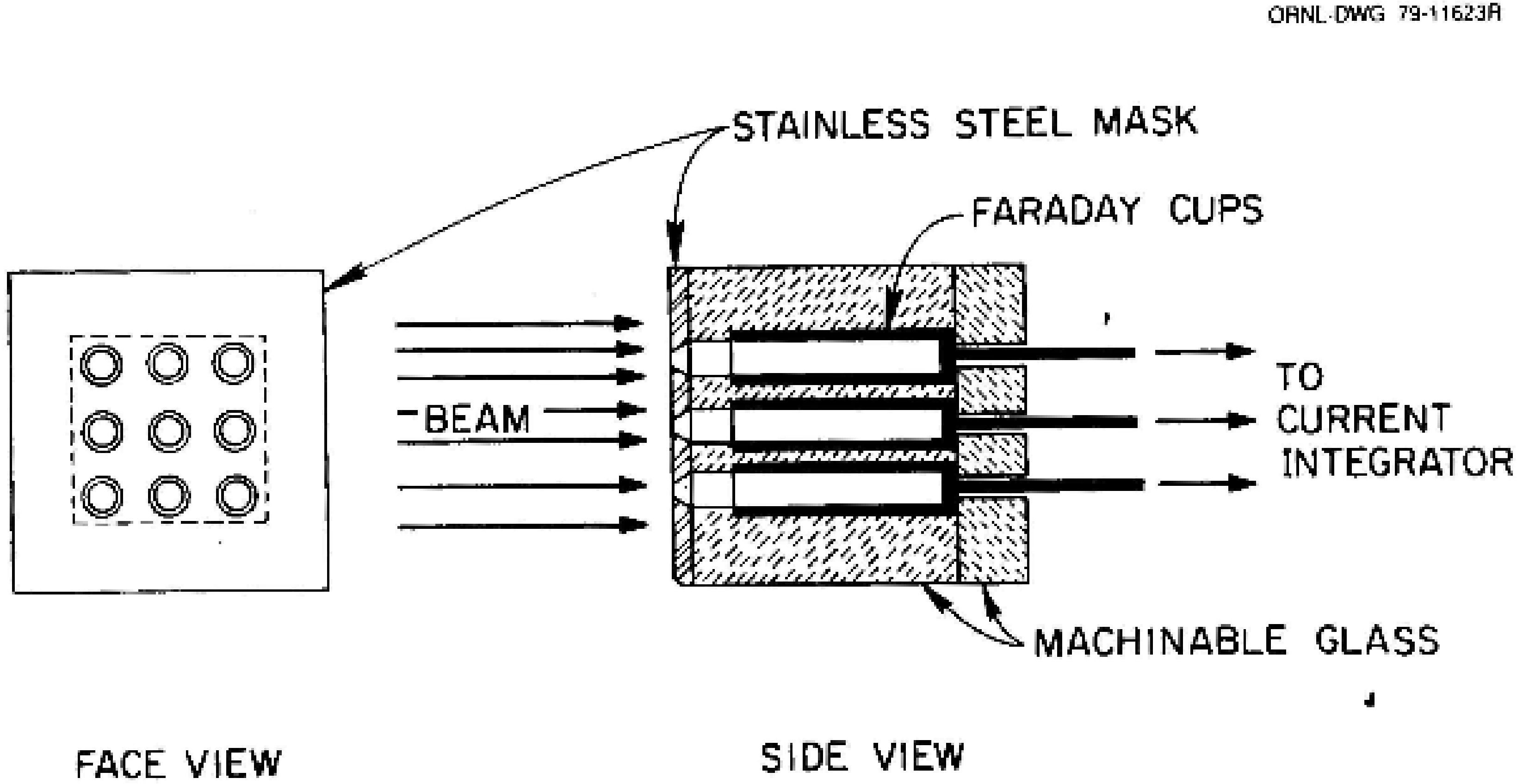

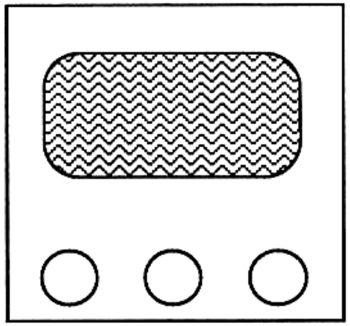

Deposition parameters

- specie
- rate
- gas pressure
- bombardment flux, energy
- angle
- number of atoms/cluster

Properties

- hardness
- toughness
- ductility
- wear
- corrosion
- oxidation
- resistivity

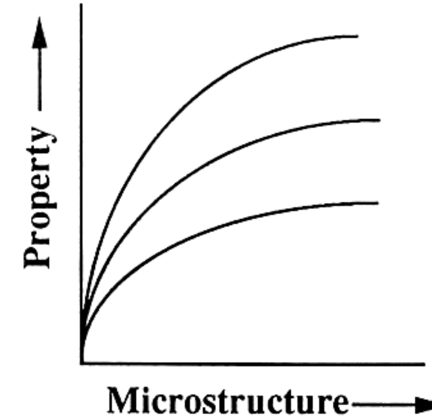

Ion Beam Assisted Deposition

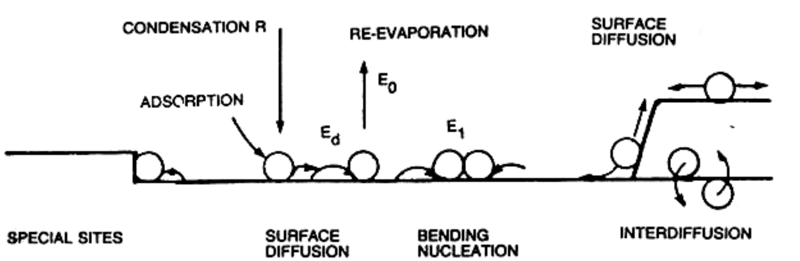

Surface Processes

- condensation
- re-evaporation
- mobility
- shadowing
- clustering
- relaxation

Microstructure

- density
- topography
- grain size, morphology
- crystallinity
- texture
- residual stress
- interface structure

Approach for controlling the interface fracture energy using Ion Beam Assisted Deposition (IBAD)

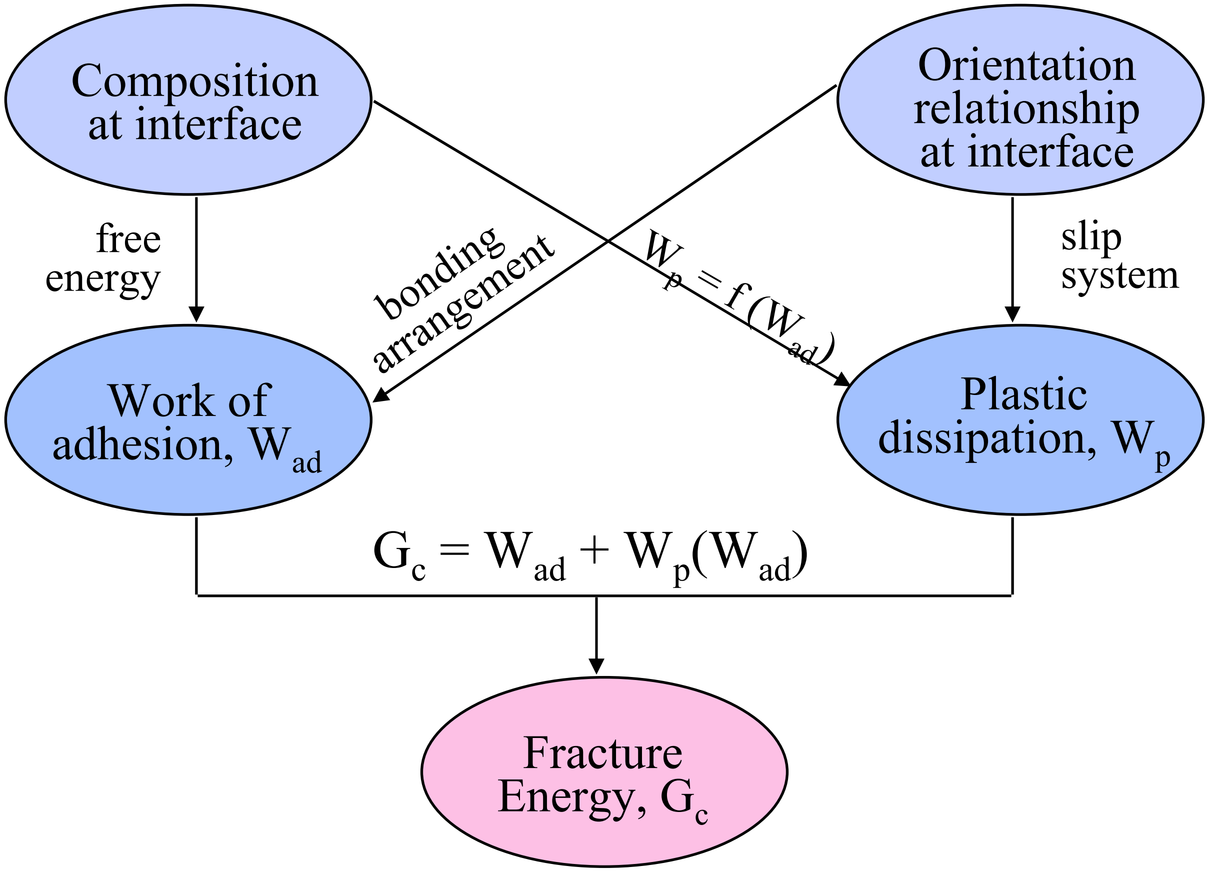

Control of orientation relationship at Nb-sapphire interface by IBAD

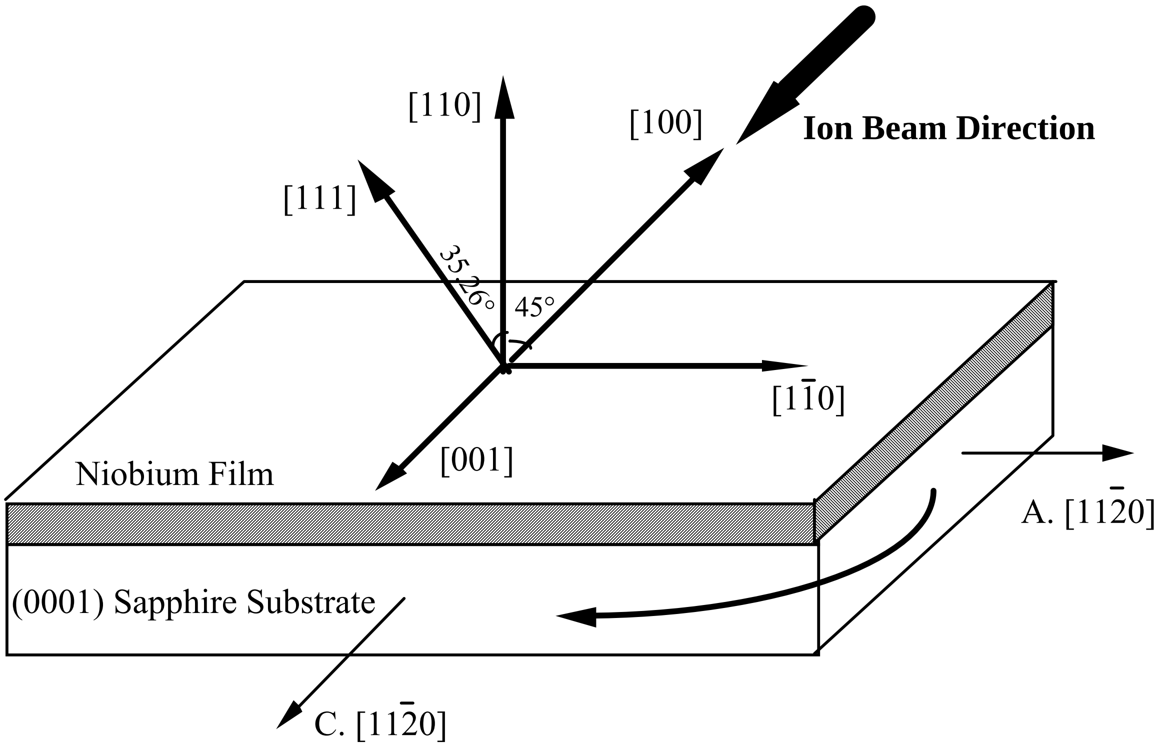

Orientation Relationships Between Niobium Film and Sapphire Substrate
A. (110) || (0001) [1$\bar{1}$0] || [11$\bar{2}$0]
C. (110) || (0001) [001] || [11$\bar{2}$0]

Schematic of Nb film growth under energetic ion bombardment

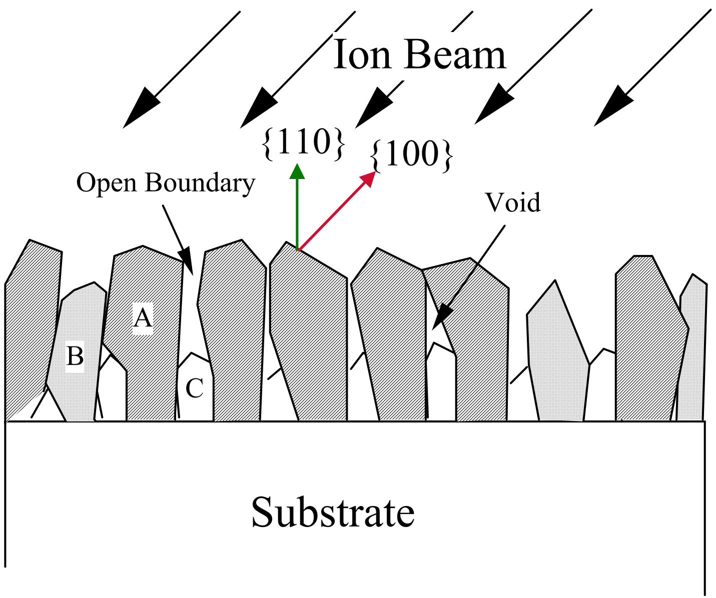

[100] channeling direction for niobium

- grain A has the easy channeling direction aligned with ion beam
- grain B and C are randomly oriented grains

Control of in-plane texture in Nb in IBAD through preferential sputtering and ion channeling

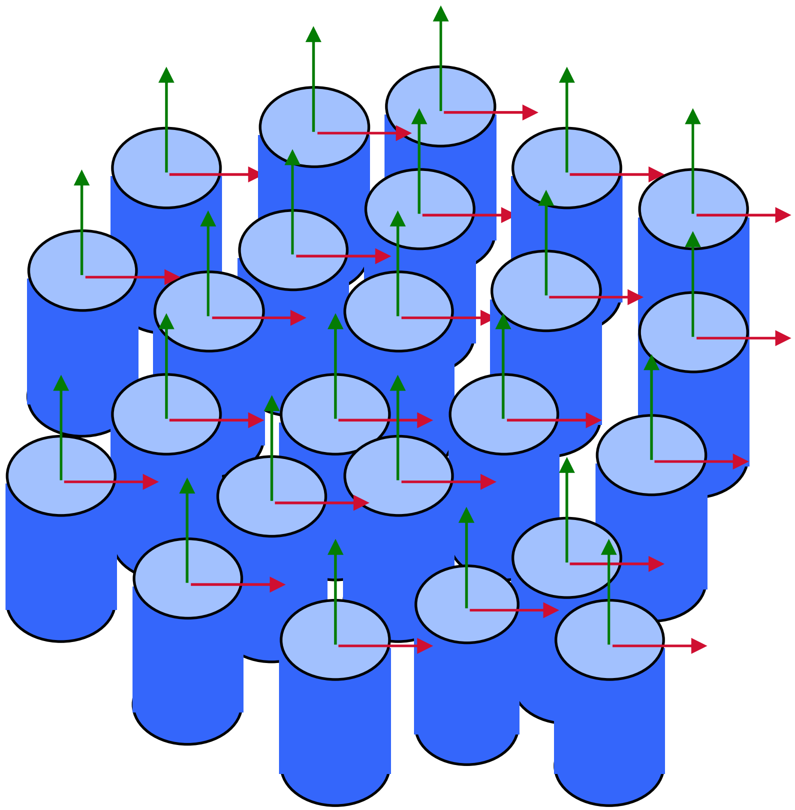

In-plane texture

Deposition of Ag and Nb onto Sapphire

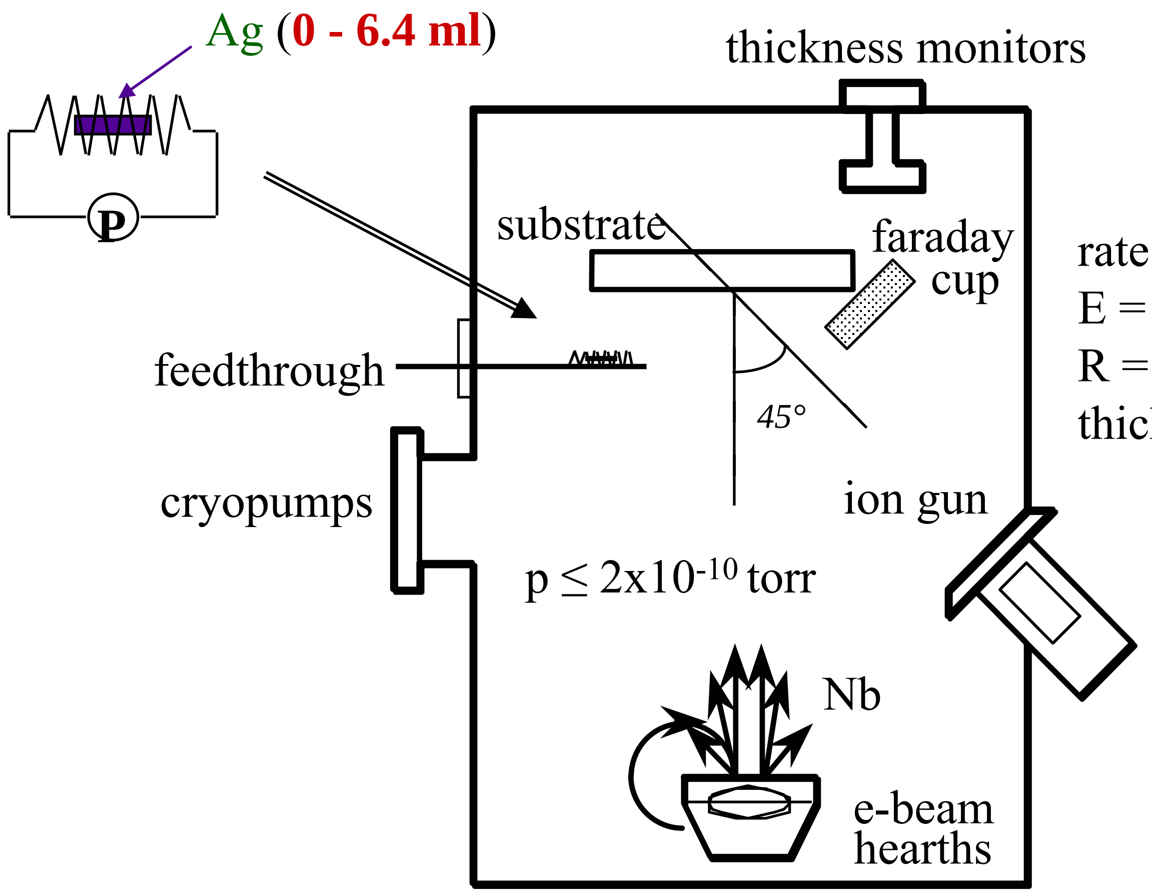

Nb

rate = 0.5 nm/s

E = 1000 eV

R = 0.4

thickness = **100-500 nm**

Buckling of patterned lines of PVD Nb on sapphire

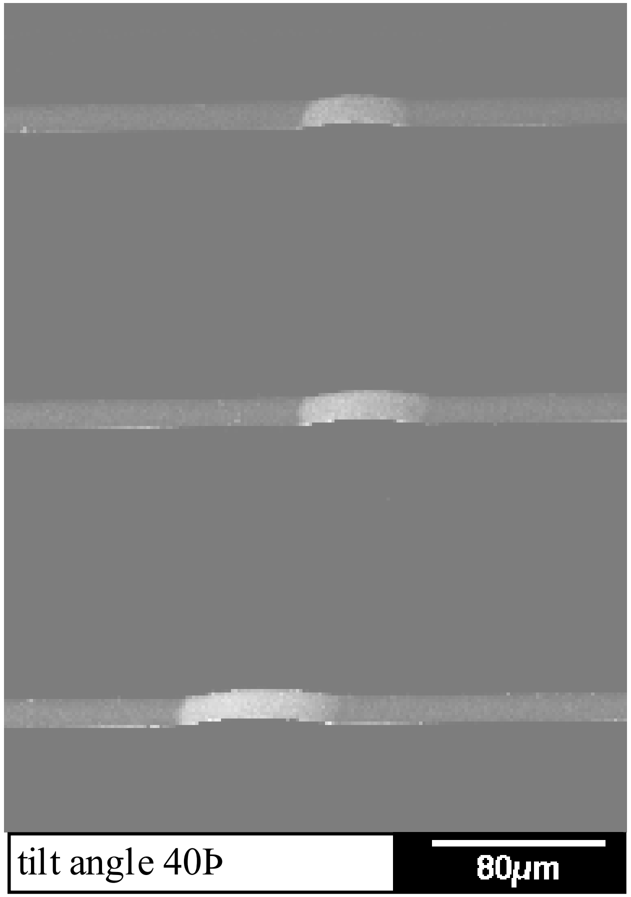

Ag: 3.0 ml

$G_c = 0.78\ J/m^2$

Nb film must be in compression

Curling of patterned lines of PVD Nb film/photoresist on sapphire

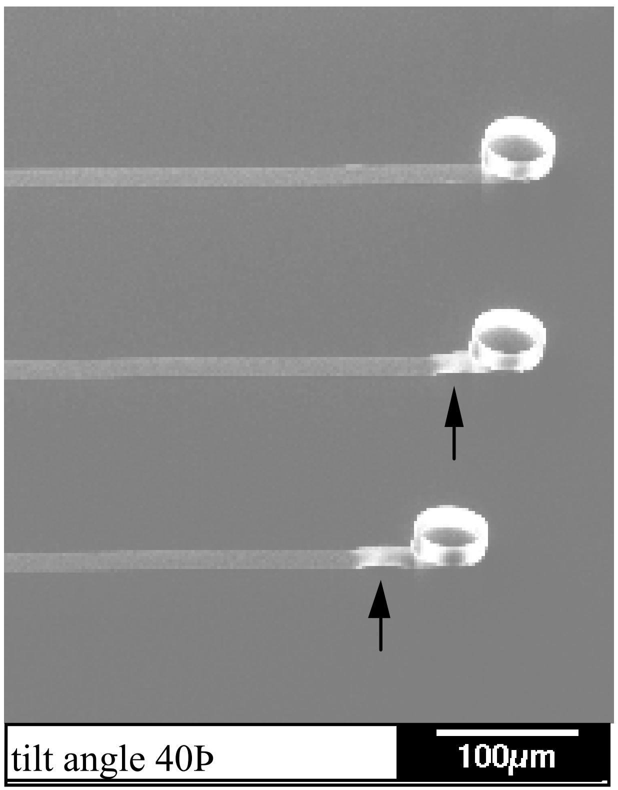

Ag: 2.1 ml

$G_c = 0.95\ J/m^2$

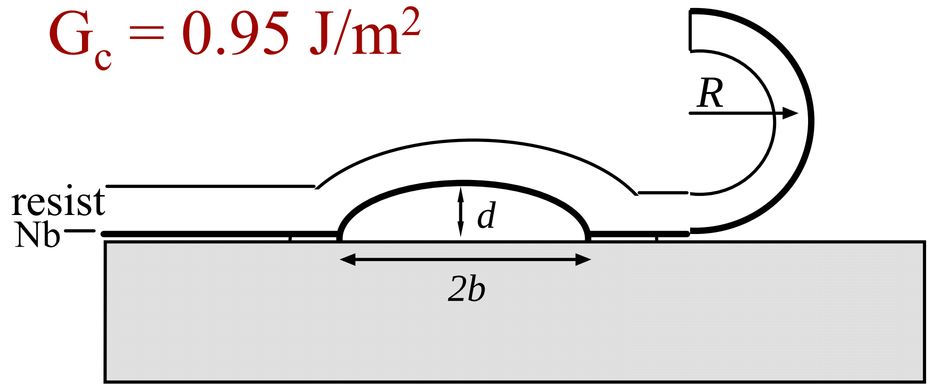

A stress gradient exists in the film/photoresist bilayer

Dispersion strengthening through IBAD

- Follstaedt, Knapp and Barbour developed use use of ion assisted deposition dispersion strengthening.

  Motivation: $\tau = 2Gb/L$ and $f \, \alpha \, (\delta/L)^3$

  20% O in Al as Al_2O_3, synthesized by ECR plasma implantation resulted in average a film hardness of ~3 GPa.

- For small (~ 1 nm), ordered precipitates, the expected strength is on the order of 5 GPa.
- Advantages over ion implantation: <u>no depth limit</u> and <u>much quicker</u>.

What we need to know

Irradiation of multilayered structures

- Layer mixing behavior at high temperatures
    - role of thermodynamics (ΔH_{mix}, ΔH_{coh})
    - role of ballistic processes and RED
- Phase formation/stability under high temperature irradiation
- Layer thickness limits
- Dose, dose rate dependence of mixing, phase stability

Synthesis of multilayered structures

- Very fine layers vs. thicker layers in hardened state
- Dispersion strengthened structures
- What about dispersion strengthened multilayer structures?